The University of Maine
DigitalCommons@UMaine

Electronic Theses and Dissertations | Fogler Library

Spring 5-15-2018

PI3K/AKT Signaling Activates HSF1 to Preserve Proteostasis and Sustain Growth

Zijian Tang
zijiantang.tang@gmail.com

Follow this and additional works at: https://digitalcommons.library.umaine.edu/etd

 Part of the Cancer Biology Commons, Cell Biology Commons, and the Developmental Biology Commons

Recommended Citation
Tang, Zijian, "PI3K/AKT Signaling Activates HSF1 to Preserve Proteostasis and Sustain Growth" (2018). *Electronic Theses and Dissertations*. 2848.
https://digitalcommons.library.umaine.edu/etd/2848

This Open-Access Dissertation is brought to you for free and open access by DigitalCommons@UMaine. It has been accepted for inclusion in Electronic Theses and Dissertations by an authorized administrator of DigitalCommons@UMaine. For more information, please contact um.library.technical.services@maine.edu.

PI3K/AKT SIGNALING ACTIVATES HSF1 TO PRESERVE PROTEOSTASIS AND SUSTAIN GROWTH

By

Zijian Tang

B.S. Wuhan University, 2006

M.S. Wuhan University, 2008

A DISSERTATION

Submitted in Partial Fulfilment of the

Requirements for the Degree of

Doctor of Philosophy

(in Biochemistry and Molecular Biology)

The Graduate School

The University of Maine

May 2018

Advisory Committee:

Chengkai Dai, Head of Proteomic Instability of Cancer Section, Advisor,

National Cancer Institute

Robert Wheeler, Associate Professor of Microbiology

Clarissa Henry, Associate Professor of Biological Sciences

Gregory Cox, Associate Professor of Biomedical Science and Engineering,

The Jackson Laboratory

MaryAnn Handel, Professor of Medicine, The Jackson Laboratory

PI3K/AKT SIGNALING ACTIVATES HSF1 TO PRESERVE PROTEOSTASIS AND SUSTAIN GROWTH

By

Zijian Tang

Dissertation Advisor: Dr. Chengkai Dai

An Abstract of the Dissertation Presented
in Partial Fulfillment of the Requirements for the
Degree of Doctor of Philosophy
(in Biochemistry and Molecular Biology)
May 2018

Signaling through oncogenic PI3K/AKT kinase pathway is crucial to cell and organ growth. Phosphorylation by AKT has long been perceived as a key factor to enhance protein biosynthesis that enables cell growth and survival. Here, we report that HSF1, the master regulator of the proteotoxic stress response (PSR), is a new AKT substrate. Beyond mobilizing the PSR under heat shock, the AKT-mediated HSF1 activation supports robust growth. In a mouse model of human megalencephaly, expression of a constitutively active *PI3KCA* suffices to drive brain overgrowth, and strikingly, it also provokes proteomic chaos including protein aggregation and amyloidogenesis. Deletion of *Hsf1* in this

model reduces the brain size and prolongs the mice survival. Furthermore, HSF1 maintains mitochondrial proteome homeostasis and prevents cell death by protecting the key mitochondrial chaperone HSP60 from aggregation. Independently of its transcriptional activity, HSF1 sequesters amyloid oligomers away from HSP60 through physical interactions. Together, our findings unveil three novel aspects of HSF1 biology: 1) HSF1 is a new substrate of AKT kinase; 2) HSF1 supports tissue overgrowth by balancing the protein quality and quantity; 3) HSF1 not only prevents amyloidogenesis but also suppresses amyloid-induced cellular toxicity.

TABLE OF CONTENTS

LIST OF FIGURES

CHAPTER 1

INTRODUCTION

1.1 Proteome Homeostasis and Human Diseases

Proteome homeostasis (proteostasis) is a process that regulates the balance of cellular production, folding, and degradation of proteins within or outside the cells (Klaips, Jayaraj et al., 2018). It maintains cellular fitness by coordinating multiple interconnected pathways to control the fate of proteins starting from biosynthesis, to folding, and to degradation (Labbadia and Morimoto, 2015). Several key players have been known to maintain proteostasis. For instance, molecular chaperones or heat shock proteins (HSPs) are the main effectors to facilitate protein biosynthesis and protein folding (Kim, Hipp et al., 2013). The ubiquitin-proteasome system controls degradation of misfolded or unfolded proteins (Bett, 2016). The autophagy and lysosome pathways are responsible for clearing protein aggregates (Tanaka and Matsuda, 2014). All these pathways cooperate with each other to maintain proteostasis and to keep cellular fitness. However, a variety of environmental challenges, such as extreme temperature, deprivation of nutrients and exposure to toxins or radiation, can disrupt proteostasis and elicit proteotoxic stress in cells (Klaips, Jayaraj et al., 2018). Constant perturbation of proteostasis can manifest in human pathologies including

neurodegenerative disorders, diabetes and cancer (Kaushik and Cuervo, 2015). For instance, failure of proteostasis can lead to accumulation of amyloid plaques and neurofibrillary tangles in brains, which are generally considered as the pathological hallmarks of Alzheimer's disease (Scheper, Nijholt et al., 2011). It is thought that disruption of proteostasis increases protein misfolding and aggregation and exhausts the proteostatic mechanisms, leaving susceptible proteins –such as Aβ amyloids in Alzheimer's disease–at a greater risk for aggregation and amyloidogenesis (Regitz, Fitzenberger et al., 2016). During amyloidogenesis, certain misfolded proteins first form the intermediate structure soluble amyloid oligomers, which can further form insoluble amyloid fibrils with enriched β-sheet structures (Gremer, Scholzel et al., 2017). Recent studies suggest that soluble oligomers of Aβ are more cytotoxic than insoluble Aβ fibrils, which contribute to neuronal cell death and cognitive decline in Alzheimer's disease patients. Researchers found that the level of Aβ oligomers is elevated in cerebrospinal fluids and cortexes of the brains of Alzheimer's disease patients (Georganopoulou, Chang et al., 2005). Furthermore, Aβ oligomers induce neuronal cell death when they are introduced into the brains of aging rhesus monkeys (Geula, Wu et al., 1998).

Disruption of proteostasis is a common characteristic of neurodegenerative disorders. Besides Alzheimer's disease, aggregation of specific proteins in degenerating brains is also found in Parkinson's disease, Huntington's disease and amyotrophic lateral sclerosis (ALS) (Fernandez-Busquets, 2013). Ubiquitous accumulation of aggregated proteins, such as Aβ-amyloid, α-synuclein and superoxide dismutase 1 (SOD1), in these diseases highlights the significance of proteostasis in neurodegenerative disorders (Ancsin, 2003).

In addition, there is growing evidence implicating the decline of proteostasis as one of the contributors to the pathogenesis of diabetes. For instance, increased protein ubiquitination and reduced proteasomal activity is detected in the islets of type 2 diabetic patients (Bugliani, Liechti et al., 2013). Furthermore, dysregulation of chaperone network is detected during the progression of diabetes, which further promotes insulin resistance, loss of beta cell differentiation and apoptosis of beta cells (Chien, Aitken et al., 2010) (Chung, Nguyen et al., 2008) .

Emerging evidence also reveals that proteotoxic stress is a novel hallmark of cancer (Donnelly and Storchova, 2015). Tumor cells need a high proteostatic capacity for basic survival and proliferation, since genetic instability within tumor cells and acid and hypoxic microenvironment outside tumor cells

constantly put them under proteotoxic stress conditions. For example, aneuploidy increases protein burden and numerous genetic mutations cause protein instability, which exacerbates the proteostasis imbalance (Sansregret and Swanton, 2017). Inhibitors that disrupt proteostasis, such as HSP90 inhibitors or proteasome inhibitors were shown to decrease tumor cell proliferation in animal models, and are currently in clinical trials for cancer therapy, which supports the importance of proteostasis to malignant transformation (Yang, Lee et al., 2017) (Kim, Lee et al., 2017). These studies have revealed a novel perspective of cancer. Much effort has been put to understand the mechanism and regulation of proteostasis in cancer. Full appreciation of the role of proteostasis will help us develop novel and improved cancer chemotherapeutics.

1.2 HSF1 is a Guardian of Proteostasis under Stress

Molecular chaperons or Heat shock proteins (HSPs) are the main effectors to maintain proteome homeostasis (Morimoto, 2011). A small group of transcriptional factors named HSFs are controlling the induction of molecular chaperones or HSPs during proteotoxic stress conditions. There are nine HSFs paralogs – HSF1, 2, 3, 4, 5, X1, X2, Y1 and Y2 – identified in vertebrates (Akerfelt, Morimoto et al., 2010). All the HSF proteins share three conserved functional domains: the N-terminal DNA binding domain (DBD), the trimerization domain enriched for hydrophobic heptad repeats (HR) and the C-terminal transactivation domain (AD) (Vihervaara and Sistonen, 2014). HSFs bind to the heat shock element, an evolutionarily conserved DNA sequence consisting of a series of nTTCnGAAn via their DBDs under proteotoxic stress conditions (Huang, Wu et al., 2018). Among these HSFs, HSF1 is the master regulator of HSP induction in mammals. Genetic ablation of *Hsf1* in MEFS abolish the induction of Hsps under proteotoxic stress conditions while deletion of *Hsf2, Hsf3, Hsf4* in mice retain the Hsps induction, which highlights HSF1's essential role in preserving proteostasis under stress conditions (Dai and Sampson, 2016).

Deletion of *Hsf1* in mice causes prenatal lethality, due to placental defects, and female infertility (Dai and Sampson, 2016). Recent study showed that *Hsf1* deficiency affects systemic body temperature regulation by increasing core body temperature (Ingenwerth, Noichl et al., 2016). In addition, sperms of *Hsf1* knockout mice lose motility after exposed to hyperthermia (Dai and Sampson, 2016).

Although there are no other disease-related phenotypes caused by proteotoxicity are detected in *Hsf1* knockout mice under normal conditions, one group found that *Hsf1* knockout mice had a significantly shortened lifespan compared to wide-type mice after infected with Rocky Mountain Laboratory (RML) prions (Steele, Hutter et al., 2008). However, surprisingly, the onset of pathological changes was observed at the same time in *Hsf1* knockout and wide-type mice, which indicates that HSF1 has a protective role in the progression of prion disease (Steele, Hutter et al., 2008). Furthermore, in another adult-motor neuron disease mouse model – spinal and muscular atrophy (SBMA) caused by the expression of CAG repeats in the androgen receptor (AR) gene, HSF1 levels are highly correlated with the accumulation of pathogenic AR. High levels of pathogenic AR are detected in the spinal motor neurons with decreased HSF1 expression. More importantly, deletion of *Hsf1* in this SBMA mice model intensifies the accumulation of pathogenic AR and aggravates neurodegeneration phenotypes (Kondo, Katsuno et al., 2013). Similarly,

Hsf1 deficiency in a Huntington's disease mouse model accelerates disease progression by increasing aggregation of mutant huntingtin (mHTT), whereas over-expression of a constitutively active form of HSF1 in the same mouse model ameliorates mHTT aggregation and extends mice lifespan (Hayashida, Fujimoto et al., 2010) (Fujimoto, Takaki et al., 2005). In a mouse model of Parkinson disease, *Hsf1* is deleted in the midbrains of mice expressing α-synuclein (Kim, Wang et al., 2016). In contrast to *Hsf1* deficiency, over-expression of a constitutively active form of HSF1 in the human cells modeling Parkinson disease reduces cellular toxicity by decreasing α-synuclein aggregation (Liangliang, Yonghui et al., 2010). Regarding Alzheimer's disease, HSF1 level is reduced in cerebellar Purkinje cells, a brain cell type that is decreased in Alzheimer's disease patients and mouse model of Alzheimer's disease. Over-expression of a constitutively active form of HSF1 in the mouse model of Alzheimer's disease recovers the cognitive defects associated with Alzheimer's disease by reducing Aβ-amyloid aggregation and restoring the number of cerebellar Purkinje cells (Jiang, Wang et al., 2013). Moreover, activation of HSF1 pharmacologically by HSP90 inhibitors decreases Aβ-amyloid aggregation and alleviates memory loss in a mouse model of Alzheimer's disease (Chen, Wang et al., 2014). Similar to Alzheimer's disease, HSF1 activity is diminished in the motor neurons of amyotrophic lateral sclerosis (ALS) patients and the mouse

model of ALS (Batulan, Shinder et al., 2003). Further deletion of *Hsf1* in a mouse model of ALS escalates aggregation of TDP-43, which is also associated with ALS in addition to SOD-1, and exacerbates the ALS-associated phenotypes, whereas overexpression of HSF1 in this mouse model reduces cellular toxicity by preventing TDP-43 from aggregating (Chen, Mitchell et al., 2016).

Accumulated evidence has demonstrated that HSF1 promotes tumorigenesis and tumor progression. Two independent studies first sowed that genetic deletion of *Hsf1* in mice impaired tumorigenesis in *Trp53* deficient mice and chemical-induced skin carcinogenesis (Min, Huang et al., 2007) (Dai, Whitesell et al., 2007). In addition, *Hsf1* deficiency suppressed carcinogenesis caused by loss of tumor suppressor gene *Nf1* and impaired the lung metastasis in MMTV-HER2/Neu transgenic mice (Dai, Santagata et al., 2012) (Xi, Hu et al., 2012). Also, another study pointed out that HSF1 largely remained in nuclear in malignant breast cancers compared to normal breast cells, which indicates HSF1 was active in malignant tumors (Santagata, Hu et al., 2011). Furthermore, HSF1 is found to stay mainly in nuclear in many other types of cancers, including cervical cancer, colon cancer, lung cancer, pancreatic cancer, prostate cancer, and meningioma, which indicates HSF1 is highly mobilized in these cancers (Dai and Sampson, 2016). Together, HSF1 is constitutively activated in cancer cells and HSF1 activation is indispensable for

tumorigenesis and tumor progression (Liao, Xue et al., 2015) (Mendillo, Santagata et al., 2012) (Tong, Li et al., 2018). Recently, researchers started to unveil the underlying mechanisms of HSF1 activation in these cancers and how HSF1 regulates proteostasis in tumor cells.

So, these findings emphasize that HSF1 critically guards proteostasis not only in physiological conditions but also in pathological conditions such as neurodegenerative disorders and cancers. Our previous study showed inhibition of HSF1 in tumor cells elicits global protein ubiquitination, aggregation, and even more strikingly, accumulation of amyloids, which is toxic to tumor cells. However, the most important question of how HSF1 suppresses amyloidogenesis to guard proteostasis remains unanswered in the field. Does HSF1 suppress amylodogenesis through its transcriptional regulation of molecular chaperons? Or, can HSF1 suppress amyloidogenesis independent of its transcriptional activity? In this project, we start addressing these key questions.

1.3 HSF1 Activation is a Multi-step Process

Upon proteotoxic stress, HSF1 undergoes trimerization, nuclear translocation, phosphorylation, and DNA binding, leading to its activation (Akerfelt, Morimoto et al., 2010). It is commonly believed that HSF1 is repressed by HSP90 complexes under normal conditions whereas it is released from this repression after HSP90 is titrated away by misfolded proteins induced by proteotoxic stress conditions (Vihervaara and Sistonen, 2014). Following trimerization and nuclear translocation, HSF1 is phosphorylated on multiple sites by different kinases, several of which are reported to promote HSF1 activity. For instance, phosphorylation of HSF1 at S230 site by CAMK2A or DAPK increases HSF1 activity (Holmberg, Hietakangas et al., 2001). Also, phosphorylation at S320 site by protein kinase A and at S419 site by polo-like kinase 1 both activates HSF1 (Zhang, Murshid et al., 2011) (Kim, Yoon et al., 2005). Furthermore, some phosphorylation events are associated with inhibition of HSF1, including S121 phosphorylation by AMPK (Dai, Tang et al., 2015), T142 phosphorylation by CK2 (Soncin, Zhang et al., 2003), S303 phosphorylation by MAPK and S363 phosphorylation by protein kinase C (PKC) (Dai, Frejtag et al., 2000) Ultimately, HSF1 trimers bind to heat shock elements in the promote regions of *HSPs* through the N-terminal DBD. However, unlike conventional proteotoxic stress conditions, tumor cells

may directly regulate HSF1 activity through oncogenic signals. Several studies have elucidated how HSF1 is regulated by oncogenic signaling in cancer.

AMP-activated protein kinase (AMPK) is a metabolic tumor suppressor (Rourke, Hu et al., 2018). AMPK functions as an energy sensor, closely monitoring the AMP/ATP or ADP/ATP ratios in the cells (Ronnebaum, Patterson et al., 2014). When cells demand acute energy, AMPK is activated to generate more ATP by stimulating fatty acid oxidation and to inhibit anabolic processes that consume ATP (Wang, Xin et al., 2017). Thus, AMPK is a therapeutic target for metabolic diseases including type 2 diabetes (Umezawa, Higurashi et al., 2017). Of note, AMPK is activated by an upstream kinase, LKB1, which is a well-known tumor suppressor (Kone, Pullen et al., 2014). *LKB1* loss-of-function mutations have been found in many different types of cancer, including lung adenocarcinomas, squamous cell carcinomas and cervical carcinomas (Zhou, Zhang et al., 2014). AMPK is a key player in mediating the tumor-suppressive role of LKB1. In a $PTEN^{+/-}$ mouse tumor model, tumor progression is accelerated by *LKB1* mutation that decreases LKB1 level, whereas tumor progression is delayed by AMPK activators that enhance AMPK activity (Huang, Wullschleger et al., 2008). In addition, in a lymphoma mouse model

expressing transgenic c-Myc, deletion of *Ampkα1*, which is encoding for the only catalytic subunit expressed in B cells, promotes the lymphoma development (Zadra, Batista et al., 2015).

Interestingly, our recent study showed that AMPK physically interacts with and phosphorylates HSF1 at S121 site under metabolic stress (Dai, Tang et al., 2015). This phosphorylation inhibits HSF1 activity partly via impairing its nuclear translocation. Both glucose deprivation and metformin treatment block HSF1 activation by activating AMPK. Importantly, both glucose deprivation and metformin treatment diminish HSF1 activity in tumor cells, disrupting tumor proteostasis and inducing apoptosis. In contrast, knocking down *AMPK* in tumor cells enhances HSF1 activity and helps tumor cells adapt to stressful tumor micro-environments. This finding indicates that HSF1 is directly regulated by the tumor-suppressive AMPK and suggests that HSF1 activation in tumors may be partly due to loss of *LKB1* and inactivation of *AMPK*.

In addition to tumor suppressor signaling, another recent study revealed that the oncogenic RAS/MEK signaling maintains tumor proteostasis via activating HSF1. The RAS/MEK signaling cascade controls cell growth, differentiation, and survival (Zhong, 2016). Hyper-activation of this signaling pathway is frequently associated with human cancer, leading to tumor development (Martinelli, Morgillo et al.,

2017). Activating somatic mutations in the components of this signaling such as *RAS, RAF, MEK* genes are identified in nearly 30% of all human cancers (Wong, 2009).

In tumor cells, inhibition of RAS/MEK signaling inactivates HSF1 through blockade of HSF1 S326 phosphorylation, leading to protein aggregation and amyloidogenesis (Tang, Dai et al., 2015). Interestingly, it is MEK, not ERK, that directly binds to and phosphorylates HSF1 at S326 site. ERK has long been regarded as the main downstream effector of RAS/MEK signaling. Instead, MEK regulates HSF1 activity through phosphorylation of S326 site whereas ERK impairs this process through inhibitory phosphorylation of MEK at T292 and T386 sites (Tang, Dai et al., 2015). These findings unveil a novel mechanism by which tumor cells constitutively mobilize HSF1 through hyper-activation of oncogenic pathways such as RAS/MEK signaling.

Despite these novel findings, many questions about how HSF1 is constitutively mobilized in tumor cells remain. Particularly, it is still unclear whether other oncogenic pathways also directly cause constitutive activation of HSF1 within cancer cells. In this project we set out to address this important question.

CHAPTER 2

PI3K/AKT SIGNALING ACTIVATES HSF1 TO PRESERVE PROTEOSTASIS AND SUSTAIN GROWTH

2.1 Summary

Through stimulation of the mTORC1-mediated translation, PI3K/AKT signaling promotes both cellular and organismal growth. Here, we report that heat-shock factor 1 (HSF1), the master regulator of the proteotoxic stress response and a key player in maintaining proteostasis, is a new physiological substrate for AKT. Under heat stress, AKT physically interacts with HSF1, phosphorylates HSF1 at Ser230 site, and regulates HSF1 DNA binding activity. Beyond mobilizing the HSR/PSR under heat shock, the AKT-mediated HSF1 activation supports robust growth. In a mouse model of human megalencephaly, expression of a constitutively active *PI3KCA* (*PI3KCA**) suffices to drive brain overgrowth. Importantly, concurrent *Hsf1* deletion reduces brain size. Mechanistically, constitutive activation of PI3K signaling in the brains induces global protein ubiquitination and, strikingly, amyloidogenesis, including Aβ amyloids closely associated with Alzheimer's disease in humans. Furthermore, *Hsf1* deficiency markedly heightens amyloid levels. Despite elevated amyloid levels, we do not detect apparent apoptosis in *Hsf1*-proficient

brains expressing *PI3KCA**. By contrast, marked apoptosis is only induced in *Hsf1*-deficient brains expressing *PI3KCA**. Thus, our results suggest that HSF1 is necessary for robust growth by balancing both protein quantity and quality, thereby preserving proteostasis and impeding amyloidogenesis. More importantly, our data reveal that HSF1 prevents HSP60 aggregation and maintains the mitochondrial proteome homeostasis to promote the overgrowth driven by PI3K/AKT signaling. Through physical interaction, HSF1 sequesters amyloid oligomers away from HSP60, and surprisingly, HSF1 mutant lacking transcriptional activity also segregates amyloid oligomer from and rescues HSP60. Our findings unveil a novel biological function of HSF1 in guarding mitochondria proteostasis and protecting cells from the toxicity induced by amyloids.

2.2 Introduction

Cells are constantly exposed to various types of biological stressors, such as hyperthermia, nutrient deprivation, toxins, and radiation. As a result, cells initiate distinct biological responses to survive theses stressful conditions (Swan and Sistonen, 2015). Among these environmental insults, proteotoxic stressors often result in accumulation of unfolded or misfolded proteins. Proteotoxic stress is mitigated by a cellular defensive mechanism called the heat-shock response (HSR) or proteotoxic stress response (PSR) (Anckar and Sistonen, 2011). Heat-shock proteins (HSPs) or molecular chaperones act as the major effectors of the PSR or HSR, which facilitate protein folding, trafficking and degradation to maintain proteome homeostasis, or proteostasis, and ensure cell survival under proteotoxic stress conditions (Dai and Sampson, 2016).

In vertebrates, a small group of transcription factors governing the HSR/PSR are called heat-shock factors (HSFs) (Vihervaara and Sistonen, 2014). Among them, heat-shock factor 1 (HSF1) is known as the master regulator of the HSR/PSR, since mice without *Hsf1* have no induction of *Hsp* transcription under proteotoxic stress conditions (Hayashida, Inouye et al., 2006). During proteotoxic stress, HSF1 undergoes multiple steps to achieve activation, including phosphorylation, trimerization, nuclear translocation,

phosphorylation and DNA binding (Santagata, Hu et al., 2011). However, the process is still not fully understood. HSF1 binds to the genomic heat-shock elements, an evolutionarily conserved DNA sequence consisting of nTTCnGAAn, to induce *HSPs'* transcription under proteotoxic stress conditions (Vihervaara, Sergelius et al., 2013). In addition, HSF1 has been implicated in development, insulin signaling, tumor initiation and progression (Vihervaara and Sistonen, 2014). HSF1 acts as a pro-oncogenic factor and is regulated by oncogenic and tumor-suppressive signaling pathways. It has become increasingly apparent that HSF1 is indispensable to tumor cell growth and survival (Dai and Sampson, 2016). Since phosphorylation is important to HSF1 activation, recent studies unveiled that phosphorylation by oncogenic pathways contributes to HSF1 constitutive activation in tumor cells. Phosphorylation of Ser326 site of HSF1 by onco-protein MEK1 or MEK2 activates HSF1 to protect proteostasis and suppress amyloidogenesis in tumor cells (Tang, Dai et al., 2015). Also, HSF1 activation is suppressed by phosphorylation of Ser121 site mediated by the tumor-suppressive AMPK (Dai, Tang et al., 2015).

Like RAS/MEK signaling, PI3K/AKT signaling is another important oncogenic pathway controlling cell growth and survival. PI3K heterodimers, consisting of p110 catalytic and p85 regulatory subunits, and are

activated by growth factor receptor tyrosine kinases (RTKs) through phosphorylation of adaptor proteins including IRS1/IRS2 (Engelman, Luo et al., 2006). Phosphorylation of these adaptor proteins releases the inhibitory effect of the p85 regulatory subunit on the p110 catalytic subunit, which allows PI3K heterodimers translocate to the plasma membrane. p110 subunit phosphorylates phosphatidylinositol (4,5)-trisphosphate (PIP_2) to generate phosphatidylinositol (3,4,5)-trisphosphate (PIP_3). PTEN, the primary negative regulator of this signaling pathway, dephosphorylates PIP_3 to PIP_2 (Wentink, Dalm et al., 2017). PIP_3 activates AKT through PDK1, and subsequently AKT regulates hundreds of downstream targets, including GSKs, FoxO transcription factors and TSC2 to promote cell growth and survival (Manning and Toker, 2017). Particularly, AKT phosphorylates and inhibits TSC2. This AKT-mediated TSC2 inhibition subsequently activates mTOR complex 1(mTOCR1), leading to enhanced protein biosynthesis that enables cell growth and survival (Laplante and Sabatini, 2012).

Here, we report that PI3K/AKT signaling activates the HSR/PSR. AKT phosphorylates HSF1 at Ser230, leading to HSF1 activation. Although constitutive activation of PI3K/AKT signaling inevitably creates proteotoxic stress and destabilizes the proteome, HSF1 plays a critical role in mitigating amyloidogenesis and, importantly, maintaining the mitochondrial proteostasis by blocking amyloid-induced HSP60

aggregation, which prevents apoptosis to support overgrowth. To our surprise, HSF1 protects HSP60 by physically interacting with amyloid oligomers. Thus, beyond shifting the canonical view of HSF1 as a transcription factor, our findings also suggest that HSF1 physically preserves proteostasis.

2.3 Results

2.3.1 PI3K/AKT Pathway regulates the PSR

Oncogenic signaling pathways play a key role in regulating HSF1 activation through phosphorylation. For instance, MEK and ERK oppositely regulate HSF1 activation and MEK directly phosphorylates the Ser326 site of HSF1 (Tang, Dai et al., 2015). To explore whether other oncogenic pathways also regulate the HSR/PSR, we focused on PI3K/AKT signaling. First, we examined its response to heat stress in HEK293T cells (Morimoto, 1991). Exposure to heat-shock elevated the phosphorylation of AKT, the key component of PI3K/AKT signaling. Phosphorylation of both Ser473 and Tyr308 of AKT were increased, which signifies the active state of PI3K/AKT signaling pathway (Fig 1 A, B).

Figure 1. PI3K/AKT pathway regulates the PSR

(A) HS activates PI3K/AKT signaling. HEK293T cells were treated with HS at 43°C for 30min. Flow cytometry confirmed pAKT T308 and pAKT S473 levels were increased after HS (mean of the geometric means of fluorescence intensity±SD, n=3 independent experiments, Student's t test). Non-HS: non-heat shock condition. HS: heat shock condition.

(B) HS activates PI3K/AKT signaling. A2058 melanoma cells were treated with HS at 43°C for 30min. IF staining confirmed that pAKT T308 and pAKT S473 levels were increased after HS. Non-HS: non-heat shock condition. HS: heat shock condition. Scale bar is 10μm.

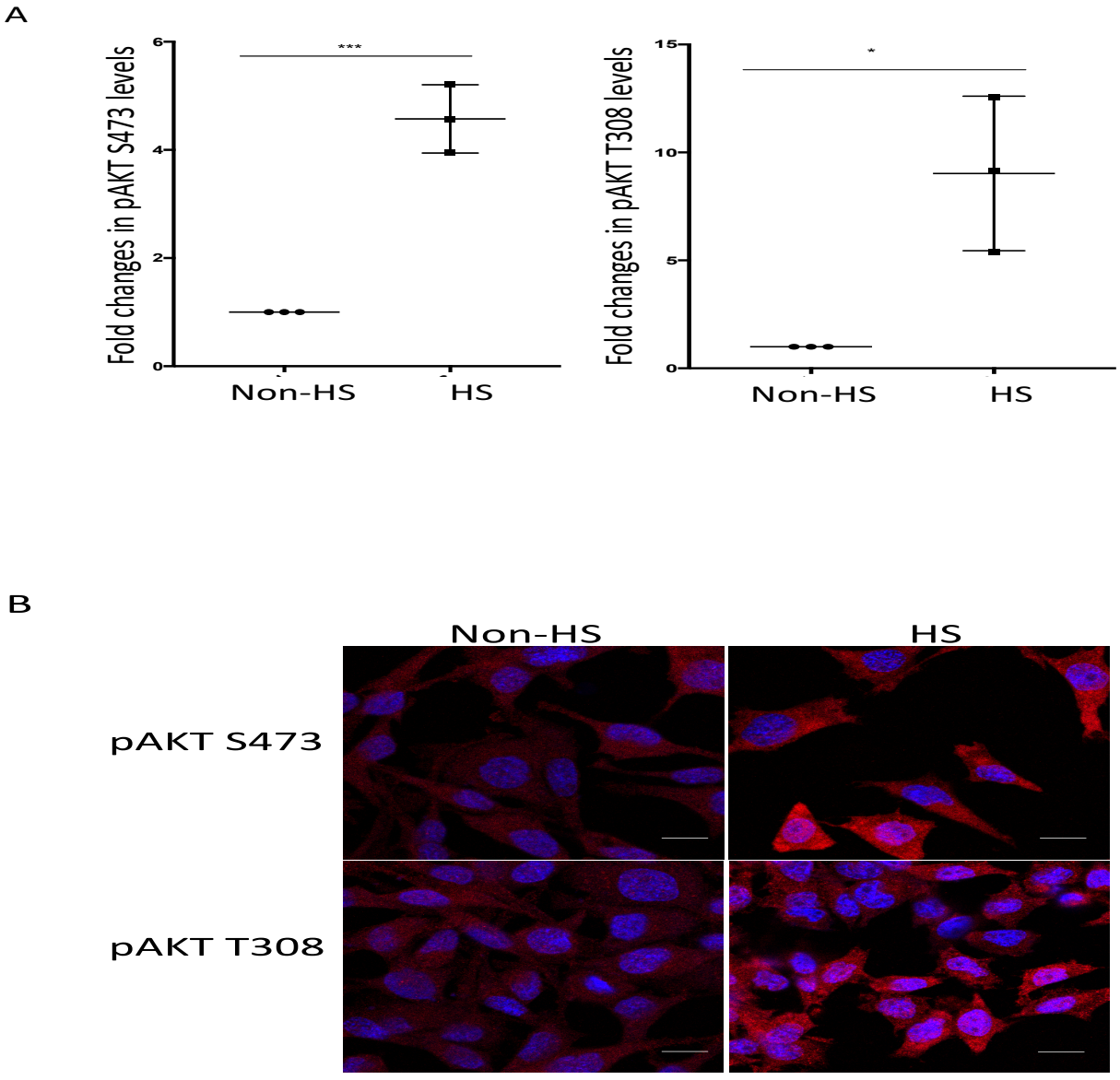

Figure 1 continued

(C) Inhibition of PI3K/AKT signaling blocks the induction of *HSPs* by HS. A2058 cells were pre-treated with 20μM LY29402 (LY), 20μM MK2206 (MK) or 20μM RG7440 (RG) for 3 hours followed by HS and 4-hr recovery at 37°C with the inhibitors. mRNA levels were quantitated by qRT-PCR (mean±SD, n=3 independent experiments, one-way ANOVA). LY: LY29402. MK: MK2206. RG: RG7440. Non-HS: non-heat shock condition. HS: heat shock condition.

(D) Inhibition of PI3K/AKT signaling blocks the induction of HSPs by HS. NIH3T3 cells stably expressing the HSE-EGFP reporter were treated with 20μM LY29402, 20μM MK2206 or 20μM RG7440 for 3 hours followed by HS and overnight recovery at 37°C with the inhibitors. Immunoblotting confirmed that protein levels of HSP72 and HSP25 were decreased after LY29402, MK2206 and RG7440 treatment during HS. LY: LY29402. MK: MK2206. RG: RG7440. Non-HS: non-heat shock condition. HS: heat shock condition.

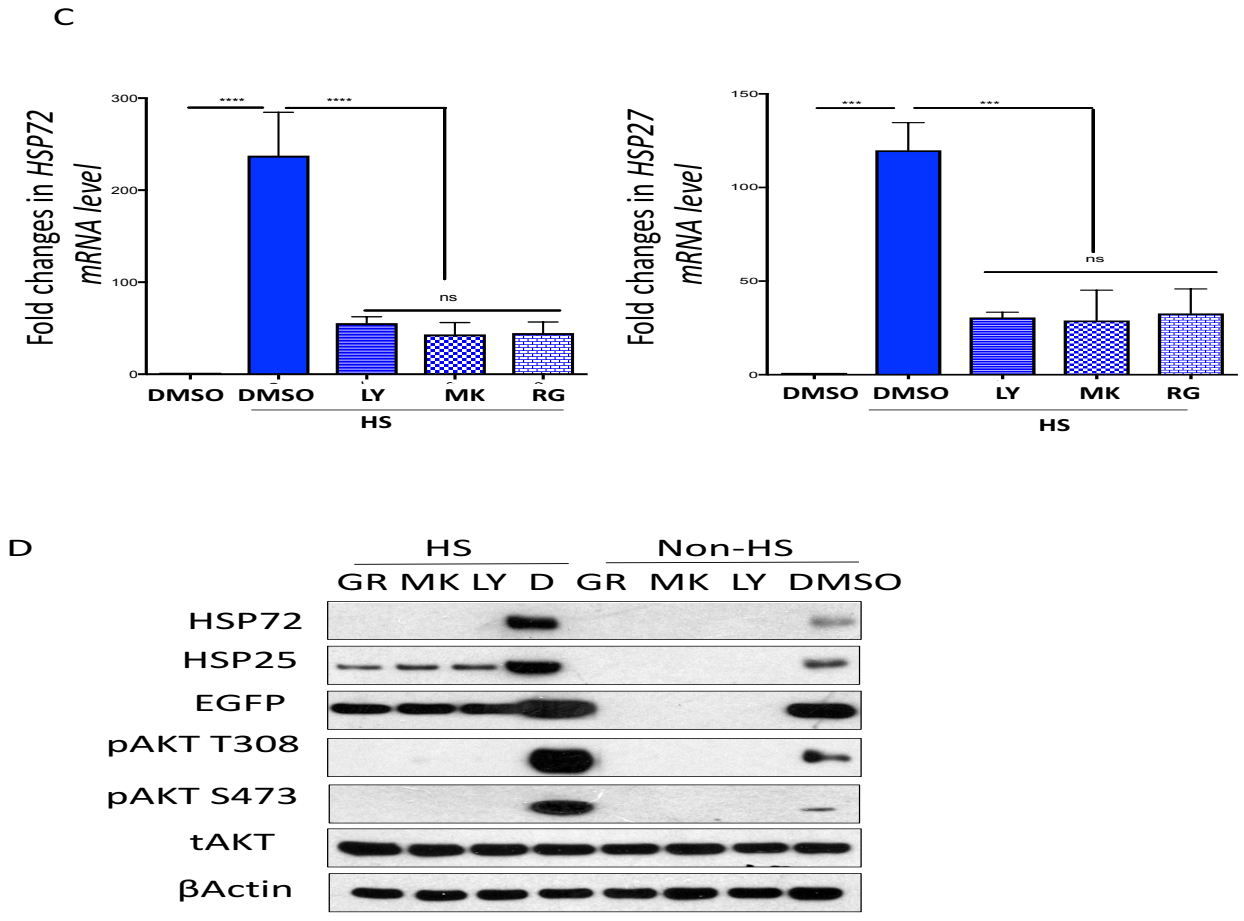

Figure 1 continued

(E) AKT1, AKT2, or AKT3 sufficiently activates HSF1. The dual HSF1 reporter system, comprising a heat shock response element (HSE)-driven secreted embryonic alkaline phosphatase (SEAP) plasmid and a CMV-driven Gaussia luciferase (GLuc) plasmid, was transfected into HEK293T cells. Cells were also transfected with constitutively active AKT1, AKT2 or AKT3 plasmids and were measured for reporter activities after 72 hours (mean ±SD, n=3 independent experiments, one-way ANOVA). Reporter assays confirmed that HSF1 was activated by constitutively active AKT1, AKT2 or AKT3.

(G) Loss of *PTEN* increases HSF1 reporter activity and this increase can be blocked by AKT inhibitors. PTEN deficient cells were transfected with the dual HSF1 reporter plasmids. After 24 hours, cells were treated with 20μM MK2206 or 20μM RG7440 for another 24 hours. Reporter assays confirmed that HSF1 reporter activities were increased in *PTEN*-deficient cells and they were suppressed by MK2206 and RG7440 treatment. (mean ±SD, n=3 independent experiments, one-way ANOVA) MK: MK2206. RG: RG7440. SCR: siControl.

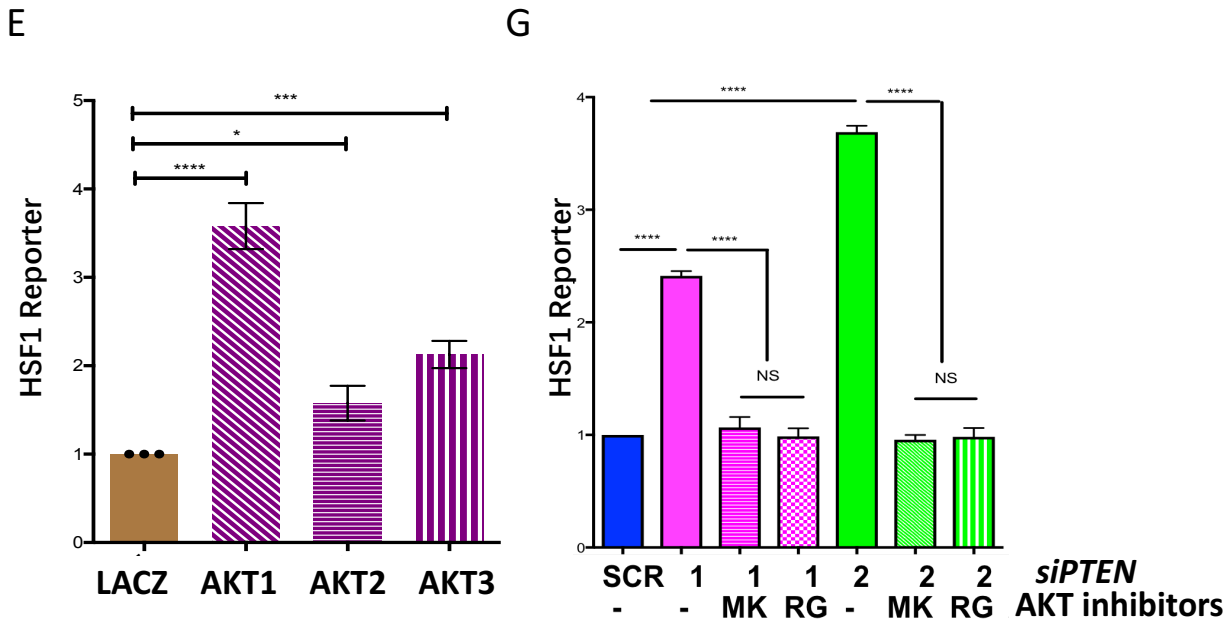

Figure 1 continued

(F) AKT1 increases the mRNA levels of *HSP72* and *HSP27*. HEK293T cells were transfected with constitutively active AKT1 plasmid for 72 hours. mRNA levels were quantitated by qRT-PCR (mean±SD, n=3 independent experiments, Student's t-test). qRT-PCR confirmed that mRNA levels of *HSP72* and *HSP27* were increased after AKT1 overexpression.

F

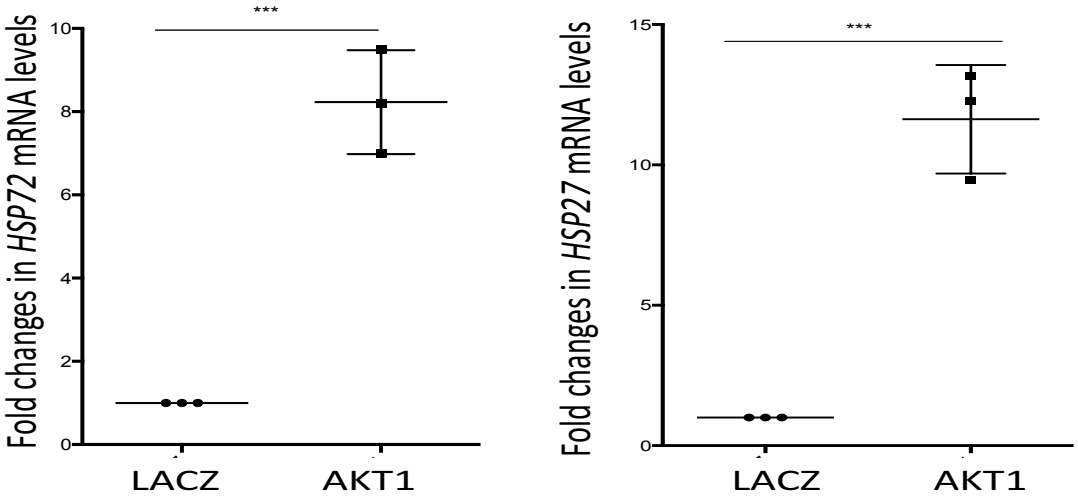

To test whether PI3K/AKT pathway regulates the HSR/PSR, we utilized MK2206 and RG7440, two specific AKT inhibitors (Winder, Unno et al., 2017) (Blake, Xu et al., 2012), and LY294002, a PI3K inhibitor (Trisciuoglio, Iervolino et al., 2005). All the inhibitors impaired the HS-induced transcription of *HSPs* genes and the production of HSP proteins (Fig 1 C, D). On the other hand, over-expression of all three isoforms of AKT (AKT1, AKT2, AKT3) proteins increased the transcriptional activity of HSF1 and mRNA levels of *HSPs* genes (Fig 1 E, F), which indicates that PI3K/AKT signaling activates the HSF1-mediated HSR/PSR and AKT directly regulates HSF1 activity. PTEN is a well-known negative regulator of the PI3K/AKT pathway (Kechagioglou, Papi et al., 2014). So, unsurprisingly, in *PTEN*-deficient cells, HSF1 activity was increased and this elevation could be suppressed by AKT inhibitors (Fig 1 G). These results further support that the PI3K/AKT signaling pathway positively regulates the HSF1 activity.

2.3.2 AKT physically interacts with HSF1 and phosphorylates Ser230 to activate HSF1

To further test whether AKT, not PI3K, directly interacts with HSF1, we carried out co-immunoprecipitation (coIP) experiments to detect endogenous interactions between AKT or PI3K and HSF1. HSF1 proteins were co-precipitated from lysates of HEK293T cells with AKT proteins, but not with PI3K proteins. Heat shock caused a markedly increased coIP of HSF1 and AKT (Fig 2 A), which demonstrates a stress-inducible AKT-HSF1 interaction. The electrophoretic mobility shift of HSF1 after heat shock suggests induced HSF1 phosphorylation (Fig 2 A). To use a different approach to examine whether HSF1 and AKT are in direct contact, we utilized the Proximity Ligation Assay (PLA) (Tang and Dai, 2017). Using two species-specific secondary antibodies conjugated with DNA oligonucleotides, PLA assay can transform protein-protein interactions in close proximity into DNA signals, which can be further detected by microscope or flow cytometry (Tang, Lu et al., 2014). We detected PLA signal in HeLa cells under both heat shock and non-heat shock conditions (Fig 2 B), whereas heat shock clearly intensified the PLA signals. These findings strongly support a direct association of HSF1 and AKT induced by heat shock.

Figure 2. AKT physically interacts with HSF1 and phosphorylates Ser230 to activate HSF1

(A) AKT physically interacts with HSF1. Endogenous HSF1 proteins were co-precipitated with AKT proteins from HEK293T cells after HS at 43°C for 30min. WCL: whole cell lysate. Immunoblotting confirmed that a direct association of HSF1 and AKT induced by heat shock. Non-HS: non-heat shock condition. HS: heat shock condition.

(B) AKT physically interacts with HSF1. Endogenous AKT1-HSF1 interactions were detected by PLA in HeLa cells using a rabbit anti-AKT1 antibody and a mouse anti-HSF1 antibody. PLA staining confirmed that a direct association of HSF1 and AKT induced by heat shock. Non-HS: non-heat shock condition. HS: heat shock condition. Scale bar is 10μm.

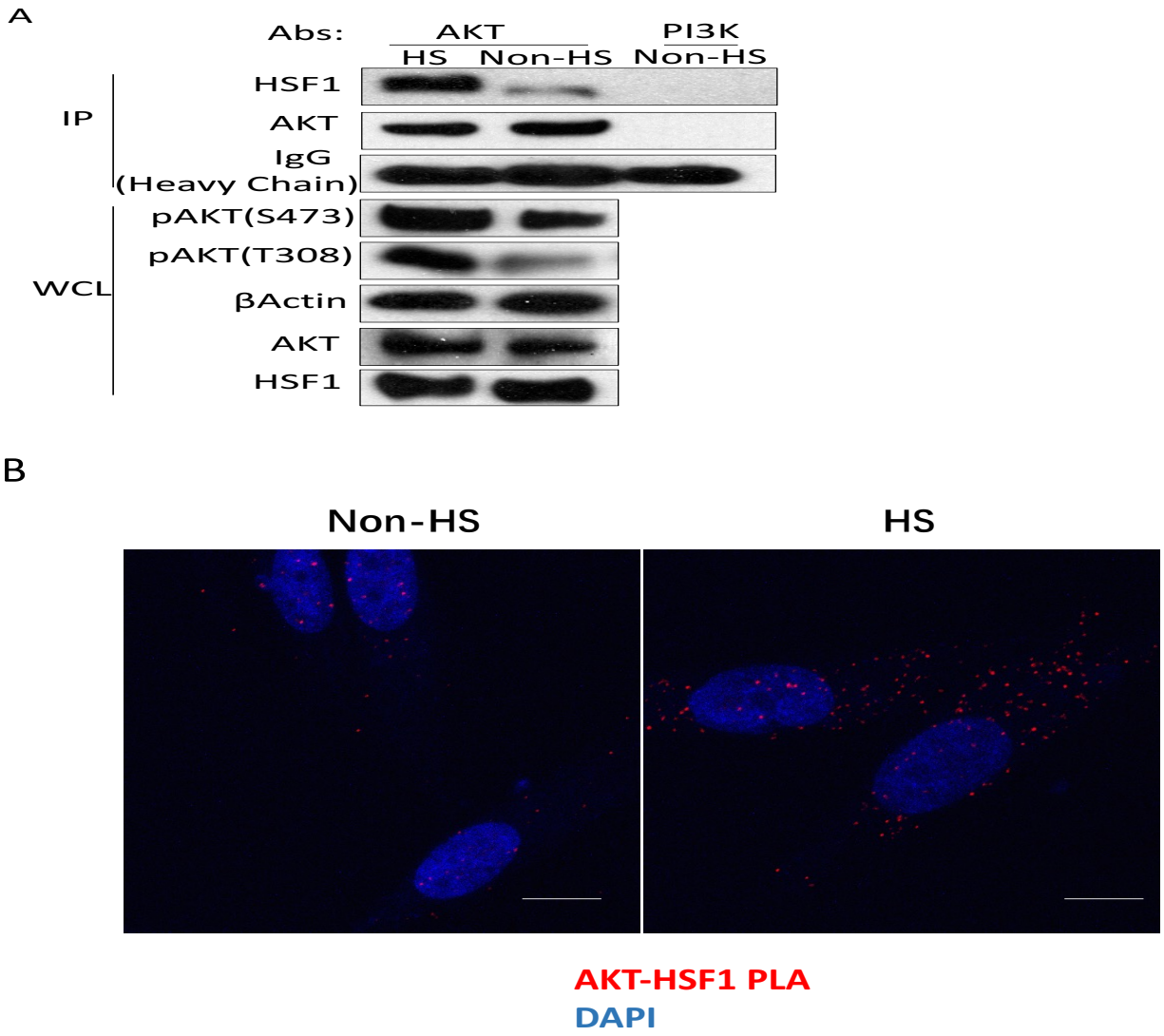

Figure 2 continued

(C) Schematic description of AKT phosphorylation motif.

(D) AKT1, AKT2 and AKT3 phosphorylate HSF1 at Ser230 site *in vitro*. 100ng recombinant AKT proteins were incubated with 400ng recombinant His-HSF1 proteins at RT for 30min. HSF1 phosphorylation was detected by immunoblotting. Blotting confirmed that AKT1, AKT2 and AKT3 proteins all phosphorylate HSF1 at Ser230 site, and MK2206 and RG7440 blocks this phosphorylation.

C

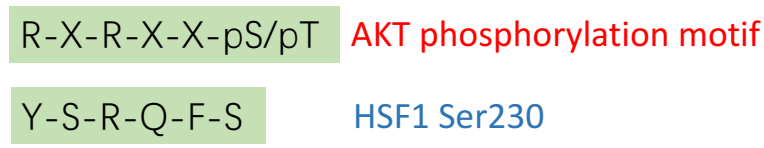

D

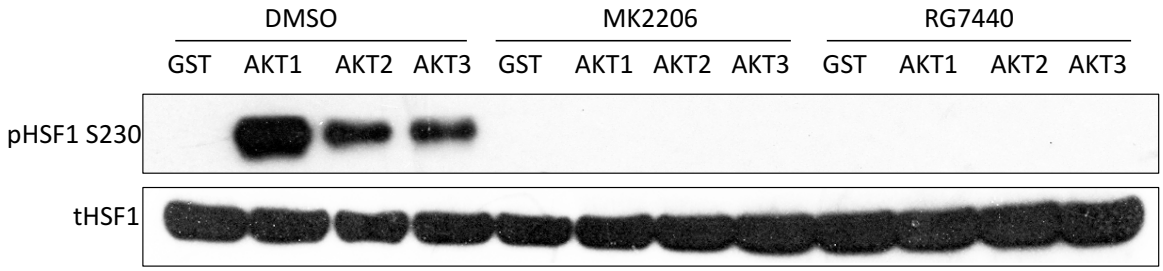

Figure 2 continued

(E) Inhibition of PI3K/AKT signaling suppresses the induction of pHSF1 S230 by HS. A2058 cells were treated with 20μM LY29402, 20μM MK2206 or 20μM RG7440 for 3 hours followed by HS and proteins were detected by immunoblotting. Blotting confirmed that levels of pHSF1 S230 were decreased after LY29402, MK2206 and RG7440 treatment under both HS and non-HS conditions. LY: LY29402. MK: MK2206. RG: RG7440. Non-HS: non-heat shock condition. HS: heat shock condition.

(F) Loss of *PTEN* increases pHSF1 S230. Proteins were detected by immunoblotting in HEK293T cells expressing *PTEN*-targeting shRNAs. Blotting confirmed that the level of pHSF1 S230 was increased in *PTEN*-deficient cells. shScram: shRNA Control.

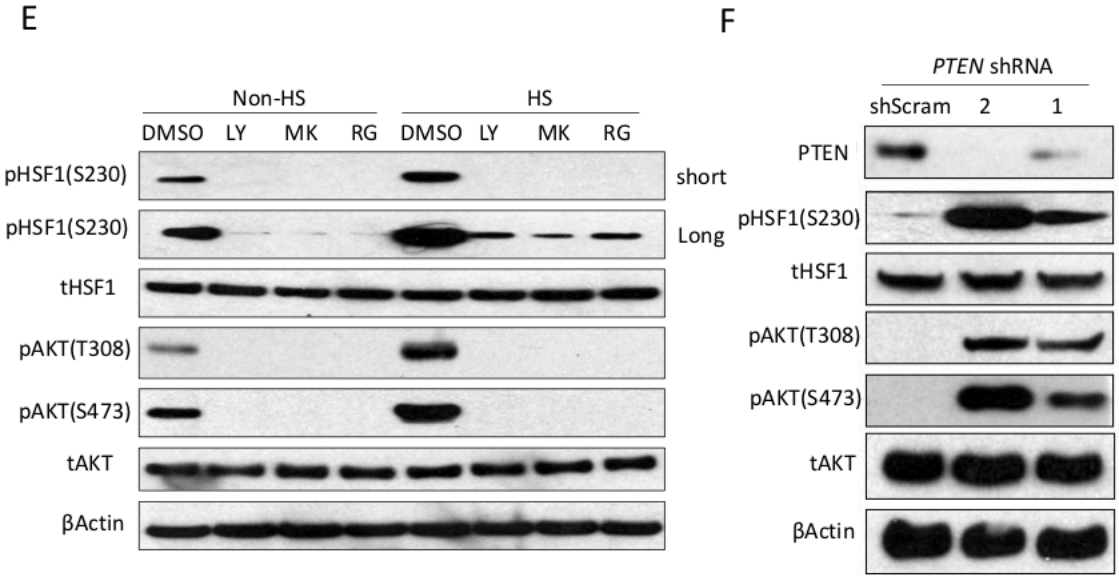

Figure 2 continued

(G) HSF1S230A mutants have impaired transcriptional activity, and AKT inhibitors impair the transcriptional activity of $HSF1^{WT}$ but not the transcriptional activity of $HSF1^{S230A}$. HEK293T cells stably expressing *HSF1*-targeting shRNAs were transfected with the dual HSF1 reporter plasmids. Cells were also co-transfected with $HSF1^{WT}$ or $HSF1^{S230A}$ plasmids and after 48 hours cells were pre-treated with 20μM MK2206 for 3 hours followed by HS and 24-hour recovery. Then cells are measured for the reporter activities (mean ±SD, n=3 independent experiments, one-way ANOVA). Reporter assays confirmed that HSF1 reporter activities were decreased in $HSF1^{S230A}$-transfected cells compared to $HSF1^{WT}$-transfected cells under both HS and non-HS conditions. HSF1 reporter activities in $HSF1^{WT}$-transfected cells but not in $HSF1^{230A}$-transfected cells were suppressed by MK2206 and RG7440 treatment. Non-HS: non-heat shock condition. HS: heat shock condition.

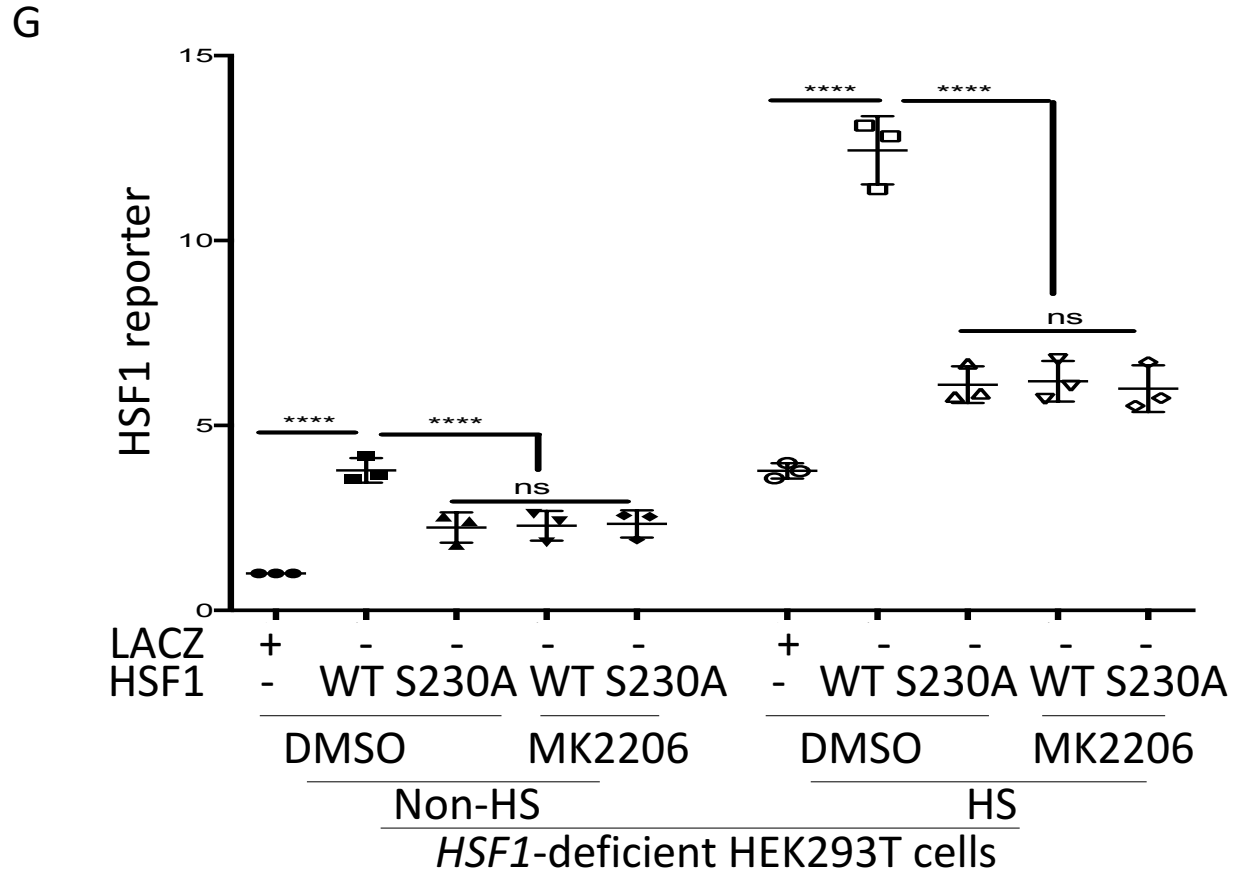

We performed bioinformatics analysis of the human HSF1 protein sequence and at residue 230 we found a putative AKT substrate motif YSRQFS (Fig 2 C). A growing body of literature has proposed that AKT phosphorylates the consensus motif R-X-R-X-X-pS/pT, where X could be any amino acid residue and pS or pT represents either phosphorylated serine or threonine (Voukkalis, Koutroumani et al., 2016). Thus, we hypothesized that AKT likely directly phosphorylates HSF1 at Ser230. In order to test this, we first incubated recombinant human HSF1 proteins with either recombinant active AKT1, AKT2 or AKT3 proteins in the presence or absence of AKT inhibitors (MK2206 and RG7440). All active AKT proteins phosphorylated HSF1 *in vitro* in the absence of AKT inhibitors, as detected by the specific pHSF1 S230 antibody, which indicates that Ser230 is an AKT phosphorylation site (Fig 2 D). We verified the specificity of this pHSF1 Ser230 antibody using *Hsf1* +/+ and -/- MEFs. Ser230 phosphorylation of HSF1 was increased in *Hsf1* +/+ MEFs cells following HS, whereas no Ser230 phosphorylation of HSF1 was detected in *Hsf1* -/- MEFs in either HS or non-HS conditions (data not shown). Either PI3K inhibitor or AKT inhibitor impaired Ser230 phosphorylation of HSF1 under both HS and non-HS conditions *in vivo* (Fig 2 E), and in *PTEN*-deficient cells, phosphorylation of HSF1 Ser230 was significantly increased

(Fig 2 F). Together, both *in vitro* and *in vivo* findings indicate that AKT directly phosphorylates HSF1 at Ser230.

Under proteotoxic stress, HSF1 undergoes a series of phosphorylation events, among which phosphorylation of Ser326 site is one key event leading to HSF1 activation (Morimoto, 2011). In contrast, how phosphorylation of Ser230 site affects HSF1 activity still remains elusive. Thus, we mutated serine 230 site to alanine and examined the transcriptional activity of this $HSF1^{S230A}$ mutant. $HSF1^{S230A}$ mutants displayed impaired transcriptional activities after transfected into *HSF1*-deficient HEK293T cells. Moreover, AKT inhibitors reduced the activity of $HSF1^{WT}$ but not the activity of $HSF1^{S230A}$ in both non-HS and HS conditions (Fig 2 G), which demonstrates that phosphorylation of Ser230 site is important for HSF1 activation by AKT.

2.3.3 PI3K/AKT Signaling regulates HSF1 DNA Binding Ability

HSF1 binding to DNA is the crucial step for HSF1 activation (Morimoto, 2014). In an effort to study whether PI3K/AKT signaling regulates HSF1 DNA-binding ability, we employed the chromatin-IP (ChIP) technique. As anticipated, HSF1 binding to both the *HSP72* and *HSP27* promoters were markedly increased following AKT1 overexpression in HEK293T cells (Fig 3 A). In contrast, both AKT inhibitors (MK2206 and RG7440) decreased HSF1 binding to the *HSP72* promoter (Fig 3 B), which demonstrates that PI3K/AKT signaling is both sufficient and necessary to regulate HSF1-DNA binding. In addition, in *PTEN*-deficient HEK293T cells HSF1-DNA binding was heightened, and this elevation was suppressed by AKT inhibitors (Fig 3 C). These results offer compelling evidence that PI3K/AKT signaling positively regulates HSF1-DNA binding. Next, we investigated the DNA binding ability of $HSF1^{S230A}$ mutants. $HSF1^{S230A}$ mutants displayed impaired binding to either the *HSP72* promoter or *HSP27* promoter after transfected into *HSF1*-deficient HEK293T cells (Fig 3 D), which indicates that phosphorylation of Ser230 site by AKT is important to the DNA binding of HSF1.

Figure 3. PI3K/AKT pathway regulates HSF1 DNA binding ability but not HSF1 nuclear translocation (A) AKT1 increases HSF1 binding to the *HSP72* and *HSP27* promoters. HSF1 ChIP assays were performed using HEK293T cells transfected with LACZ or AKT1 plasmids for 72 hours. The results were normalized against the values of IgG controls (mean ±SD, n=3 independent experiments, one-way ANOVA). qPCR confirmed that AKT1 increases HSF1 binding to the *HSP72* and *HSP27* promoters. (B) Inhibition of PI3K/AKT signaling decreases HSF1 binding to the *HSP72* promoter. ChIP assays were performed using HEK293T cells treated with 20μM MK2206 or 20μM RG7440 for overnight. The results were normalized against the values of IgG controls (mean ±SD, n=3 independent experiments, one-way ANOVA). qPCR confirmed that MK2206 and RG7440 decreases HSF1 binding to the *HSP72* promoter. (C) Loss of *PTEN* increases HSF1 binding to the *HSP72* promoter and this increase can be blocked by AKT inhibitors. HSF1 ChIP assays were performed using HEK293T cells stably expressing *PTEN*-targeting shRNAs treated with DMSO or 20μM MK2206 for overnight. The results were normalized against the values of IgG controls (mean ±SD, n=3 independent experiments, one-way ANOVA). qPCR confirmed that HSF1 binding to the *HSP72* promoter was increased in *PTEN*-deficient cells and MK2206 blocked this. MK: MK2206.

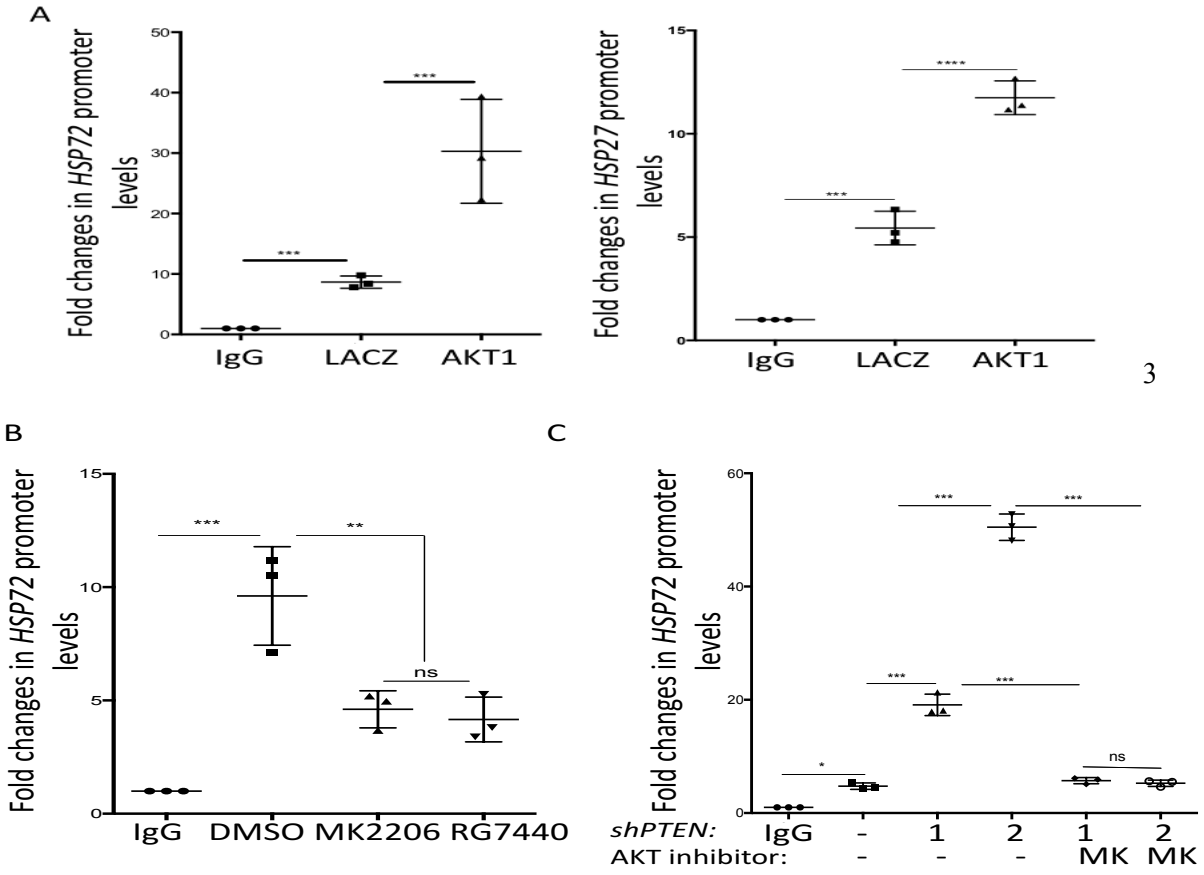

Figure 3 continued

(D) HSF1^{S230A} mutants have impaired binding ability to the *HSP72* and *HSP27* promoters. HSF1 ChIP assays were performed using *HSF1*-deficient HEK293T cells transfected with HSF1^{WT} or HSF1^{S230A} plasmids for 72 hours. The results were normalized against the values of IgG controls (mean ±SD, n=3 independent experiments, one-way ANOVA). qPCR confirmed that HSF1 binding to *HSP72 and HSP27* promoters were decreased in HSF1^{S230A} transfected HEK293T cells compared to HSF1^{WT} transfected HEK293T cells.

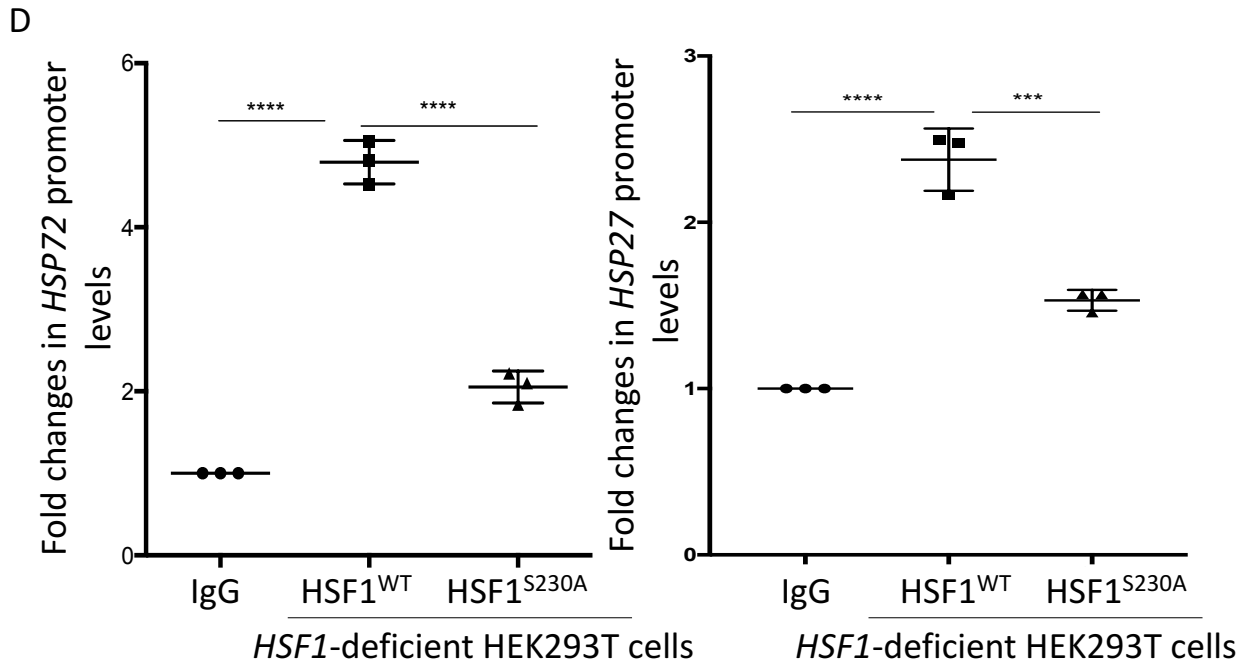

Figure 3 continued

(E) Inhibition of PI3K/AKT signaling does not affect HSF1 nuclear translocation. A2058 cells were pre-treated with 20μM LY29402 or 20μM MK2206 for 3 hours followed by HS. Blotting confirmed that LY29402 and MK2206 did not impair HSF1 nuclear translocation under both HS and non-HS conditions. LY: LY29402. Non-HS: non-heat shock condition. HS: heat shock condition. C: cytoplasmic fraction. N: nuclear fraction.

(F) $HSF1^{S230A}$ mutants have the same nuclear translocation ability as $HSF1^{WT}$. *HSF1*-deficient HEK293T cells were transfected with $HSF1^{WT}$ or $HSF1^{S230A}$ plasmids for 72 hours followed by HS. Immunoblotting confirmed that nuclear translocation of $HSF1^{S230A}$ mutants was not affected. Non-HS: non-heat shock condition. HS: heat shock condition. C: cytoplasmic fraction. N: nuclear fraction.

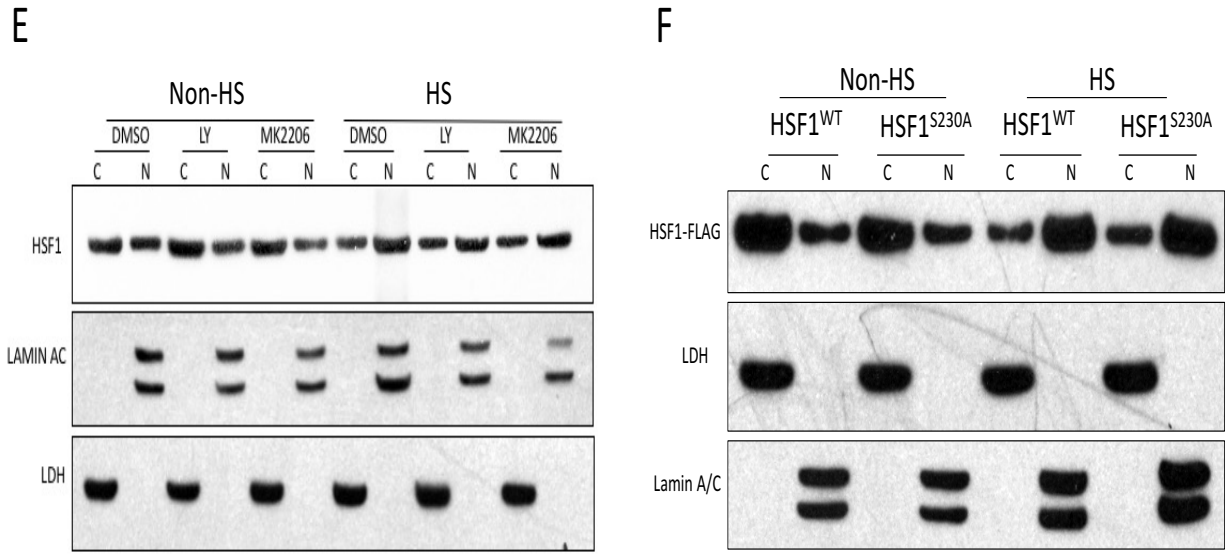

HSF1 activation is a multi-step process, including phosphorylation, nuclear translocation, and DNA binding. Next, we investigated whether PI3K/AKT pathway regulates HSF1 nuclear translocation, a prerequisite for its DNA binding. As predicted, heat shock induced HSF1 proteins to translocate from the cytoplasm to the nucleus (Fig 3 E). Interestingly, neither LY294002 nor MK2206 impeded this process (Fig 3 E). LDH and LAMIN A/C were used as the cytoplasmic and nuclear fraction marker respectively. Also, $HSF1^{S230A}$ mutants displayed normal nuclear translocation after transfected into *HSF1*-deficient HEK293T cells (Fig 3 F). Thus, we conclude that PI3K/AKT signaling positively regulates HSF1 DNA binding, but does not affect HSF1 nuclear translocation.

2.3.4 AKT competes with CaMKII and DAPK to phosphorylate HSF1

Ca2+/calmodulin-dependent protein kinase (CaMKII) and death-associated protein kinase (DAPK) have also been reported to phosphorylate HSF1 at Ser230 site (Holmberg, Hietakangas et al., 2001) (Benderska, Ivanovska et al., 2014). In order to understand how all three kinases, CaMKII, DAPK and AKT, interact with HSF1, we first tested that both CaMKII and DAPK indeed phosphorylate HSF1 at Ser230 *in vitro*. Recombinant HSF1 proteins were incubated with recombinant active CaMKII or DAPK proteins *in vitro*. Both CaMKII and DAPK proteins phosphorylated HSF1 proteins *in vitro*, as detected by the pHSF1 Ser230 antibody. (Fig 4 A) Also, phosphorylation of HSF1 by DAPK was blocked by the DAPK inhibitor (TC-DAPK 6) (Fig 4 B). In addition, knocking down either *CaMKII* or *DAPK* impaired HSF1 Ser230 phosphorylation *in vivo* (Fig 4 C D). Together, these *in vitro* and *in vivo* findings demonstrated that both CaMKII and DAPK phosphorylate HSF1 at serine 230 site. Then, we hypothesized that AKT must compete with CaMKII and DAPK to phosphorylate HSF1 at Ser230 *in vivo*. To test our theory, we utilized PLA to investigate HSF1-AKT interactions with the deficiency of either *CaMKII*, *DAPK* or both. PLA signals was measured by flow cytometry. Knocking down either *CaMKII* or *DAPK* increased the HSF1-AKT interaction, and knocking down both further intensified it (Fig 4 E),

which strongly supports that AKT competes with CaMKII and DAPK to phosphorylate HSF1 at Ser230 *in vivo*.

Figure 4. AKT competes with CaMKII and DAPK to phosphorylate HSF1

(A) Both CaMKII and DAPK phosphorylate HSF1 at Ser230 site. 100ng recombinant CaMKII or DAPK proteins were incubated with 400ng recombinant His-HSF1 proteins at RT for 30min. HSF1 phosphorylation was detected by immunoblotting. Blotting confirmed that pHSF1 Ser230 levels were increased when HSF1 proteins were incubated with either recombinant CaMKII or DAPK proteins.

(B) DAPK phosphorylate HSF1 at Ser230 site in the absence of DAPK inhibitor. 100ng recombinant CaMKII or DAPK proteins were pre-incubated with the DAPK inhibitor (TC-DAPK 6) followed by incubation with 400ng recombinant His-HSF1 proteins at RT for 30min. HSF1 phosphorylation was detected by immunoblotting. Blotting confirmed that pHSF1S230 levels were increased when HSF1 proteins were incubated with DAPK proteins and DAPK inhibitors blocked it.

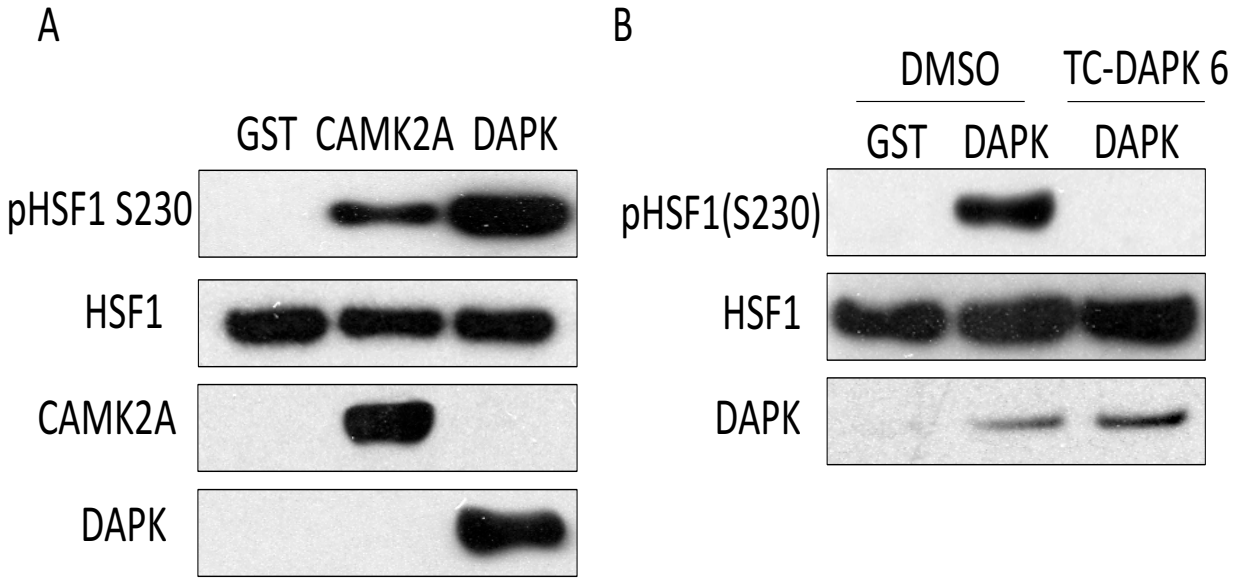

Figure 4 continued

(C) CaMKII phosphorylates HSF1 at Ser230 site in vivo. Proteins were detected by immunoblotting in HEK293T cells transfected with siRNAs targeting CaMKII. Blotting confirmed that pHSF1S230 levels were decreased following CaMKII knockdown.

(D) DAPK phosphorylates HSF1 at Ser230 site *in vivo*. Proteins were detected by immunoblotting in HEK293T cells transfected with siRNAs targeting *DAPK*. Blotting confirmed that pHSF1S230 levels were decreased following *DAPK* knockdown.

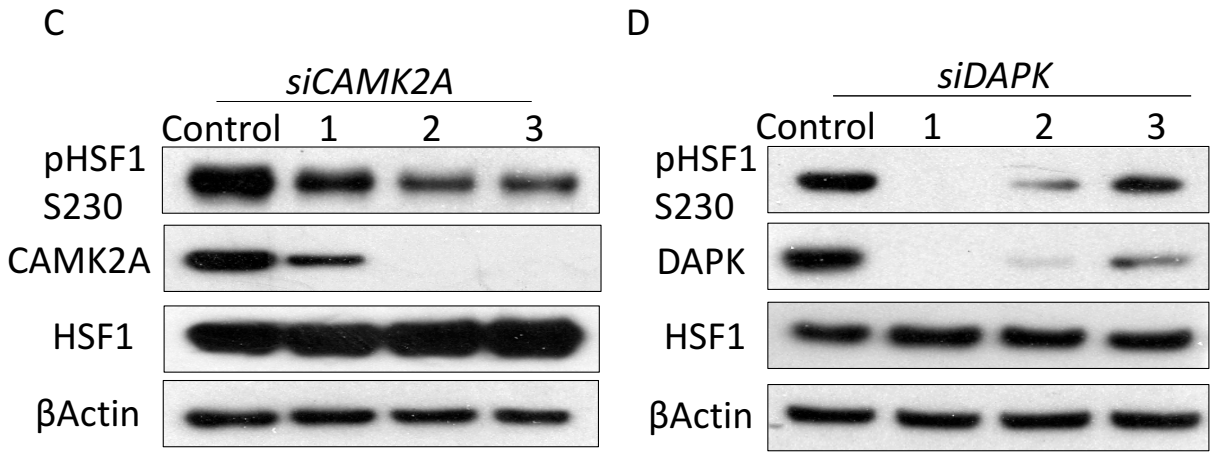

Figure 4 continued

(E) AKT competes with DAPK and CaMKII to phosphorylates HSF1 at Ser230 site in vivo. Endogenous AKT1-HSF1 interactions were detected by PLA in HEK293T cells transfected with siRNAs targeting either CaMKII, DAPK or both. PLA signals were captured by flow cytometry (mean of the geometric means of fluorescence intensity±SD, n=3 independent experiments, one-way ANOVA). Flow cytometry confirmed that association of AKT with HSF1 was enhanced when either DAPK or *CaMKII* was knocked down. Knockdown of both *DAPK* and *CaMKII* further increased the interaction between AKT and HSF1.

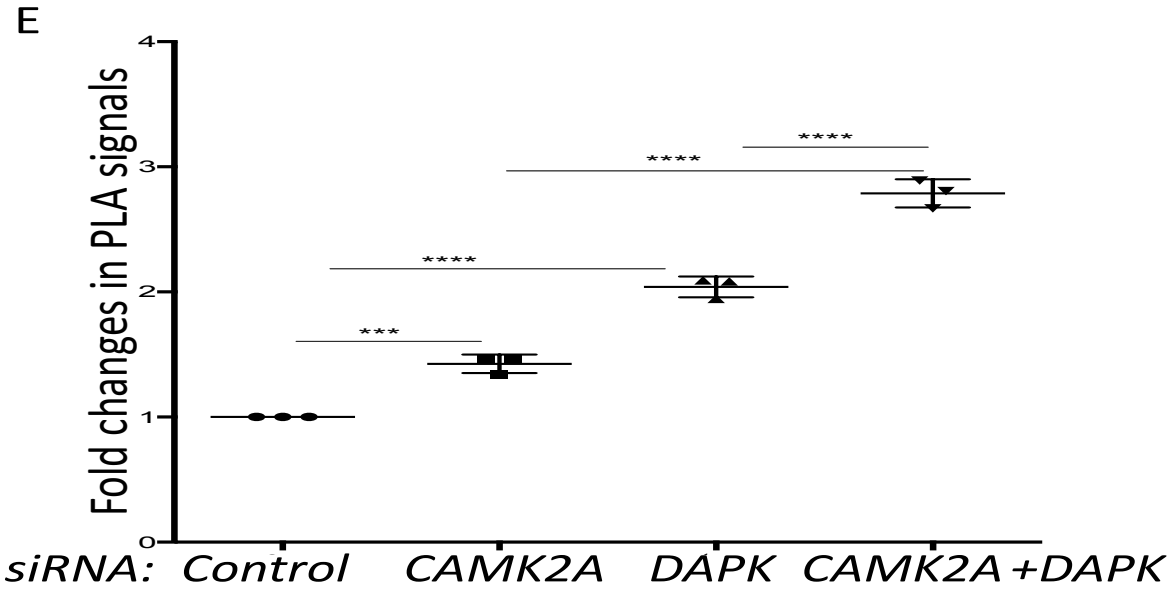

2.3.5 AKT activates HSF1 independent of MEK

Our recent study proposed that MEK phosphorylates HSF1 at Ser326 site to activate HSF1 (Tang, Dai et al., 2015). To investigate whether PI3K/AKT signaling activates HSF1 independent of RAS/MEK signaling, we examined whether RAS/MEK signaling also affects the phosphorylation of Ser230. We incubated recombinant human HSF1 proteins with recombinant active MEK1 or AKT1 proteins *in vitro*. MEK1 phosphorylated HSF1 only at Ser326 site, as detected by the specific pHSF1 Ser326 antibody, and AKT1 phosphorylated HSF1 only at Ser230 site *in vitro* (Fig 5 A). Also, both MK2206 and RG7440 impaired Ser230, but not Ser326, phosphorylation of HSF1, whereas the MEK inhibitor AZD6244 only blocked Ser326 phosphorylation of HSF1 *in vivo* (Fig 5 B). Both the *in vitro* and *in vivo* results highlight that AKT1 and MEK1 independently phosphorylated HSF1 at two different sites. Using the HSF1 reporter system, we discovered that overexpression of constitutively active AKT1 or MEK^{DD} sufficiently increased HSF1 activity and overexpression of both AKT1 and MEK^{DD} together had an additive effect on activating HSF1 under both heat-shock and non-heat shock conditions (Fig 5 C). In addition, either MK2206 or AZD6244 alone suppressed HSF1 activity, whereas a combination of both further inhibited HSF1 activity under both HS and non-HS conditions (Fig 5 D). More importantly, overexpression of $MEK1^{DD}$ activated $HSF1^{S230A}$ mutants, which cannot be activated by AKT1 (Fig 5 E); and overexpression

of AKT1, but not MEK^{DD}, increased the activity of $HSF1^{S326A}$ mutants (Fig 5 E). All these results indicate that PI3K/AKT and RAS/MEK signaling pathways regulate HSF1 activation independently.

Figure 5. AKT signaling activates HSF1 independent of MEK

(A) MEK and AKT phosphorylate HSF1 at different sites. 100ng recombinant active AKT1 or MEK1 proteins were incubated with 400ng recombinant His-HSF1 proteins at RT for 30min. HSF1 phosphorylation was detected by immunoblotting. Blotting indicated that pHSF1 S230 levels were increased when HSF1 proteins were incubated with AKT1 proteins, and pHSF1 S326 levels were increased when HSF1 proteins were incubated with MEK1 proteins.

(B) Inhibition of MEK or AKT decreases HSF1 phosphorylation at different sites. A2058 melanoma cells were treated with 20μM AZD6244, 20μM MK2206 or 20μM RG7440 for overnight. Blotting confirmed that MK2206 and RG7440 decreased pHSF1 S230 levels, and AZD6244 decreased pHSF1 S326 levels. MK: MK2206. RG: RG7440. AZD: AZD6244.

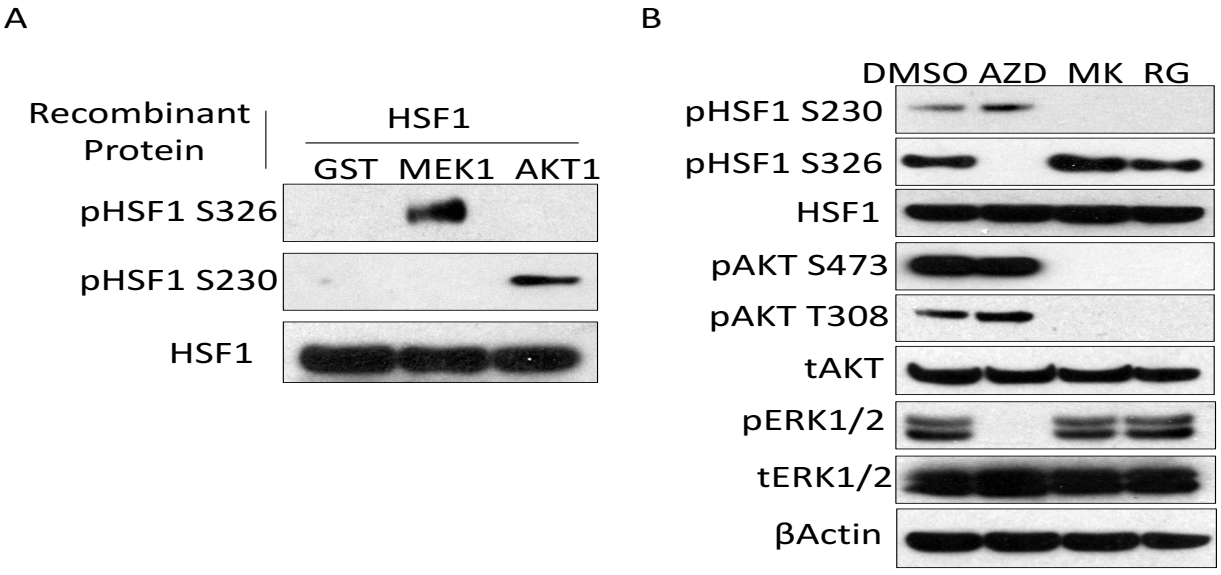

Figure 5 continued

(C) Co-expression of MEK and AKT additively increases HSF1 reporter activities. HEK293T cells were co-transfected with the dual HSF1 reporter plasmids and AKT1 or MEK^{DD} plasmids. After 48 hours, cells were measured for reporter activities (mean ±SD, n=3 independent experiments, one-way ANOVA). Reporter assays confirmed that HSF1 activity was increased in MEK^{DD}- or AKT1-transfected cells, and co-expression of both further increased HSF1 reporter activities.

(D) Combination of AKT and MEK inhibitors additively decreased HSF1 reporter activities under both HS and non-HS conditions. HEK293T were transfected with the dual HSF1 reporter plasmids. After 48 hours cells were treated with 20μM MK2206, 20μM AZD6244, or both for 3 hours followed by HS and 24-hour recovery with inhibitors. Then cells were measured for reporter activities (mean ±SD, n=3 independent experiments, one-way ANOVA). Reporter assays confirmed that the HSF1 reporter activity was decreased in AZD6244- or MK2206-treated cells, and combination of AKT and MEK inhibitors additively decreased HSF1 reporter activities. MK: MK2206. AZD: AZD6244. Non-HS: non-heat shock condition. HS: heat shock condition.

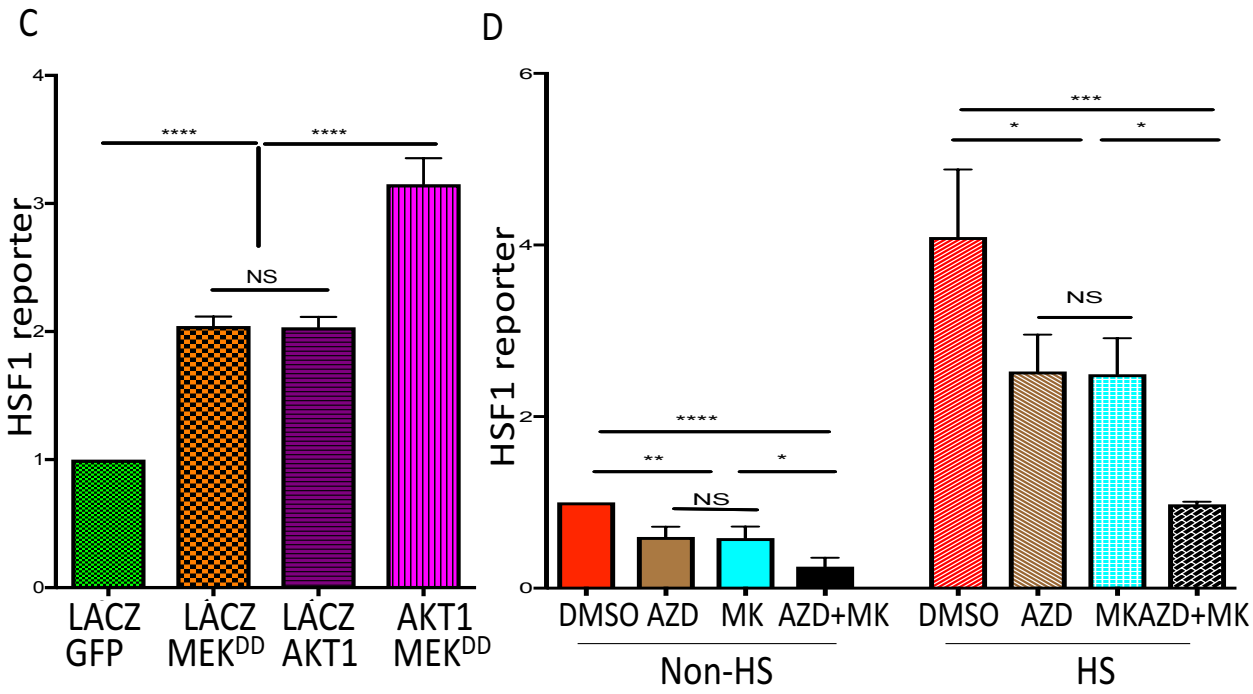

Figure 5 continued

(E) AKT or MEK activates different HSF1 mutants. *HSF1*-deficient HEK293T cells were transfected with the dual HSF1 reporter plasmids and AKT1, MEK^{DD}, $HSF1^{S326A}$ or $HSF1^{S230A}$ plasmids. After 48 hours, cells were measured for reporter activities (mean ±SD, n=3 independent experiments, one-way ANOVA). Reporter assays confirmed that the activity of $HSF1^{S230A}$ was increased by MEK^{DD} expression and the activity of $HSF1^{S326A}$ was increased by AKT1 expression.

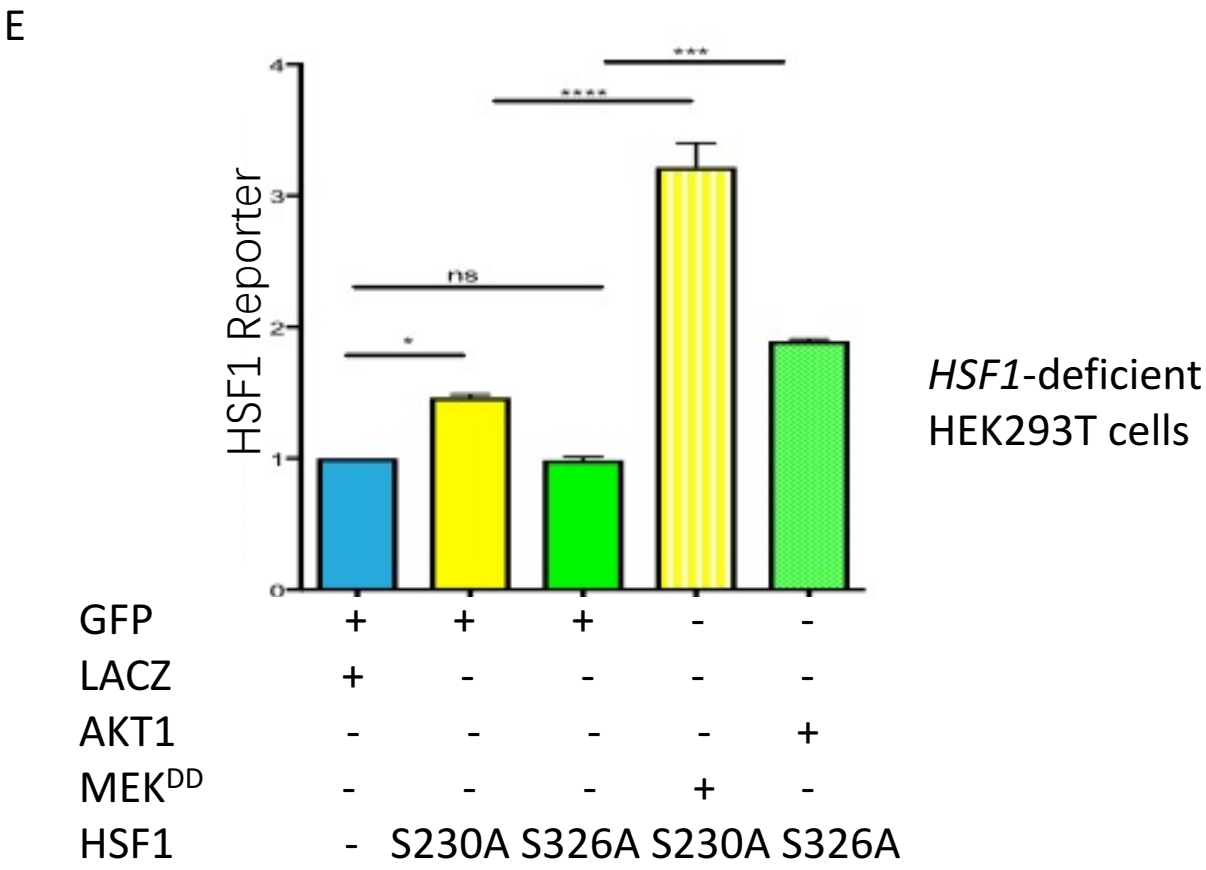

2.3.6 PI3K/AKT Signaling activates HSF1 to support Tissue Overgrowth

Since PI3K/AKT signaling plays a critical role in controlling cell and tissue growth, we wondered whether HSF1 activation could facilitate the PI3K/AKT-driven growth *in vivo*. To constitutively activate PI3K/AKT signaling *in vivo*, we used *R26Stop^{FL}P110** mice. These mice express a conditional constitutively active *PI3KCA* allele from the *ROSA26* locus. In this conditional allele, a *STOP* cassette flanked by *loxP* sites prevents the transcription of the constitutively active *PI3KCA* chimera, *p110**, and *EGFP* (Srinivasan, Sasaki et al., 2009) (Fig 6 A). When crossed with Cre deleter mouse strains, this *p110** allele can be expressed in a tissue-specific manner. In addition to human cancers, activating mutations of the components of PI3K/AKT signaling have been implicated in human megalencephaly (Riviere, Mirzaa et al., 2012), a developmental disorder characterized by brain overgrowth. As a result, patients of megalencephaly have abnormally larger brains than the general population (Mirzaa, Riviere et al., 2013). To date, no mouse models for human megalencephaly have been generated.

To model human megalencephaly and study tissue overgrowth in mice, we crossed *R26Stop^{FL}P110** mice with *hGFAP-Cre* mice. In this model, expression of the *p110** sufficed to drive brain overgrowth, leading to rapid demise after birth, since *hGFAP-Cre* selectively activated PI3K/AKT signaling in multi-potential neural stem cells (Zhuo, Theis et al., 2001). To examine the effect of *Hsf1* in this model, we further

crossed *R26Stop^{FL}P110* (PI3K p110*)* mice with *Hsf1$^{fl/fl}$* and *hGFAP-Cre* mice to produce *PI3K p110$^{*+;}$ Hsf1$^{+/+}$;Cre^{+}, PI3K p110^{*-};Hsf1$^{fl/fl}$;Cre^{+}, PI3K p110^{*+};Hsf1$^{fl/fl}$;Cre^{+},* and *PI3K p110^{*-};Hsf1$^{+/+}$;Cre^{+}* genotypes. So, *p110** will be expressed and *Hsf1* will be deleted in the same *hGFAP*- expressing cells, including both astrocytes and neurons. *PI3K p110^{*-};Hsf1$^{+/+}$;Cre^{+}* mice serve as the controls for the effects of constitutive activation of PI3K, and these mice have normal brain size (Fig 6 B). *PI3K p110^{*+};Hsf1$^{fl/fl}$;Cre^{+}* and *PI3K p110^{*+};Hsf1$^{+/+}$;Cre^{+}* mice were tested for the effects of *Hsf1* on growth driven by constitutively active PI3K. All *PI3K p110^{*+};Hsf1$^{+/+}$;Cre^{+}* mice developed enlarged brains compared to control mice (Fig 6 B). In contrast, *PI3K p110^{*+}* mice with homozygous *Hsf1* deletion showed significantly reduced brain size (Fig 6 B). All these results indicate that *Hsf1* is important for cell and tissue overgrowth driven by PI3K/AKT signaling.

Figure 6. PI3K/AKT signaling activates HSF1 to support tissue overgrowth

(A) Schematic description of *R26StopFLP110* (PI3K p110*)* mice, *Hsf1*$^{fl/fl}$ mice and *hGFAP-Cre* mice.

(B) Constitutively active PI3K/AKT signaling drives brain overgrowth. Mouse brains from four distinct genotypic groups were compared. Pictures confirmed that *PI3K p110**$^{+}$*;Hsf1*$^{+/+}$*;Cre*$^{+}$ mice have overgrown brains, and deletion of *Hsf1* reduced brain size.

(C) Schematic description of *Pten*$^{fl/fl}$ mice, *Hsf1*$^{fl/fl}$ mice and *Albumin-Cre* mice.

(D) Loss of *Pten* drives liver overgrowth. Livers of mice were compared. Pictures confirmed that *Pten*$^{fl/fl}$*;Hsf1*$^{+/+}$*;Cre*$^{+}$ mice have overgrown livers, and deletion of *Hsf1* reduced liver size.

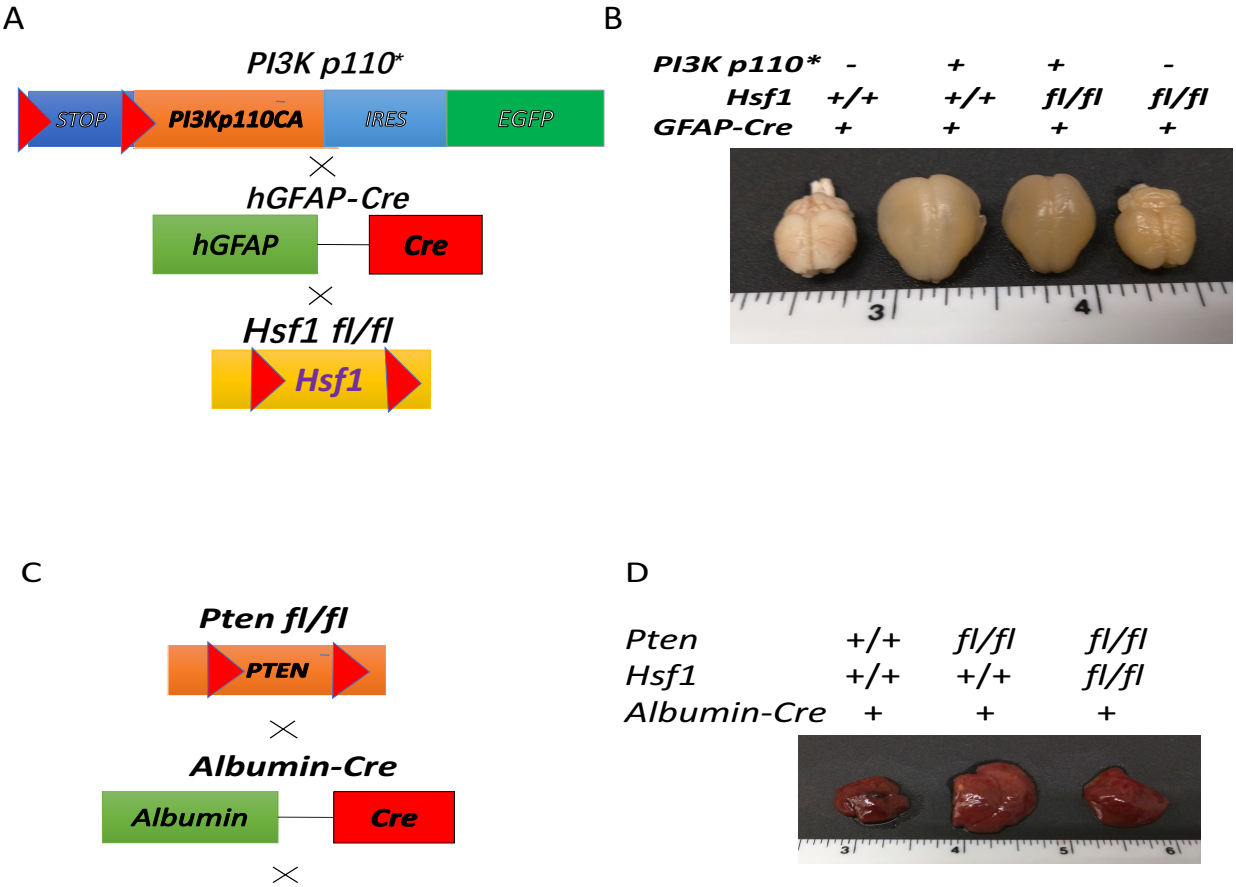

Figure 6 continued

(E) HSF1 suppresses amyloidogenesis induced by constitutively active PI3K/AKT signaling. Amyloid fibrils in mouse brains were quantified by ELISA using the OC antibody (mean±SD, n=5 brains, one-way ANOVA). ELISA confirmed that PI3K/AKT signaling elevated amyloid fibril levels in the brains, and deletion of Hsf1 further increased it.

(F) HSF1 suppresses cell death in overgrown brains. Caspase 3 activities were detected in mouse brains (mean±SD, n=5 brains, one-way ANOVA). Cell death was only detected in Hsf1-deficient overgrown brains.

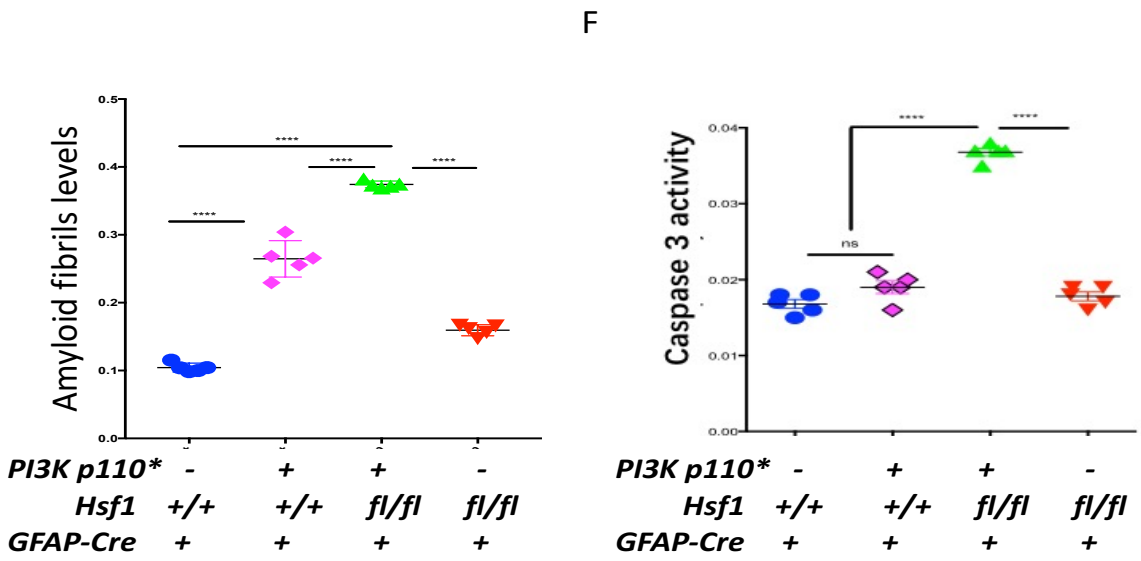

Figure 6 continued

(G) Constitutively active PI3K/AKT signaling drives amyloidogenesis by enhancing protein translation. Following treatments with 20μM LY25804702, a potent p70S6K inhibitor, and the pan-caspase inhibitor Z-VAD-FMK for overnight, amyloid oligomers and amyloid fibrils were quantitated by ELISA in primary astrocytes (mean±SD, n=3 lines of astrocytes, one-way ANOVA). ELISA confirmed that the S6K inhibitor decreased amyloid oligomers and fibrils levels in *p110*$^{+}$;Hsf1$^{+/+}$;Cre^{+} and p110*$^{+}$;Hsf1$^{fl/fl}$;Cre^{+}* astrocytes.

(H) Inhibition of amyloidogenesis reduces cell death. Following treatments with 10μM Congo Red for overnight, amyloid fibrils and Caspase 3 activity were quantitated in primary astrocytes (mean±SD, n=3 lines of astrocytes, one-way ANOVA). ELISA confirmed that Congo red decreased amyloid oligomers and fibrils levels in *p110*$^{+}$;Hsf1$^{+/+}$;Cre^{+} and p110*$^{+}$;Hsf1$^{fl/fl}$;Cre^{+}* astrocytes. Congo red treatment also reduced caspase 3 activity in *p110*$^{+}$;Hsf1$^{+/+}$;Cre^{+} and p110*$^{+}$;Hsf1$^{fl/fl}$;Cre^{+}* astrocytes.

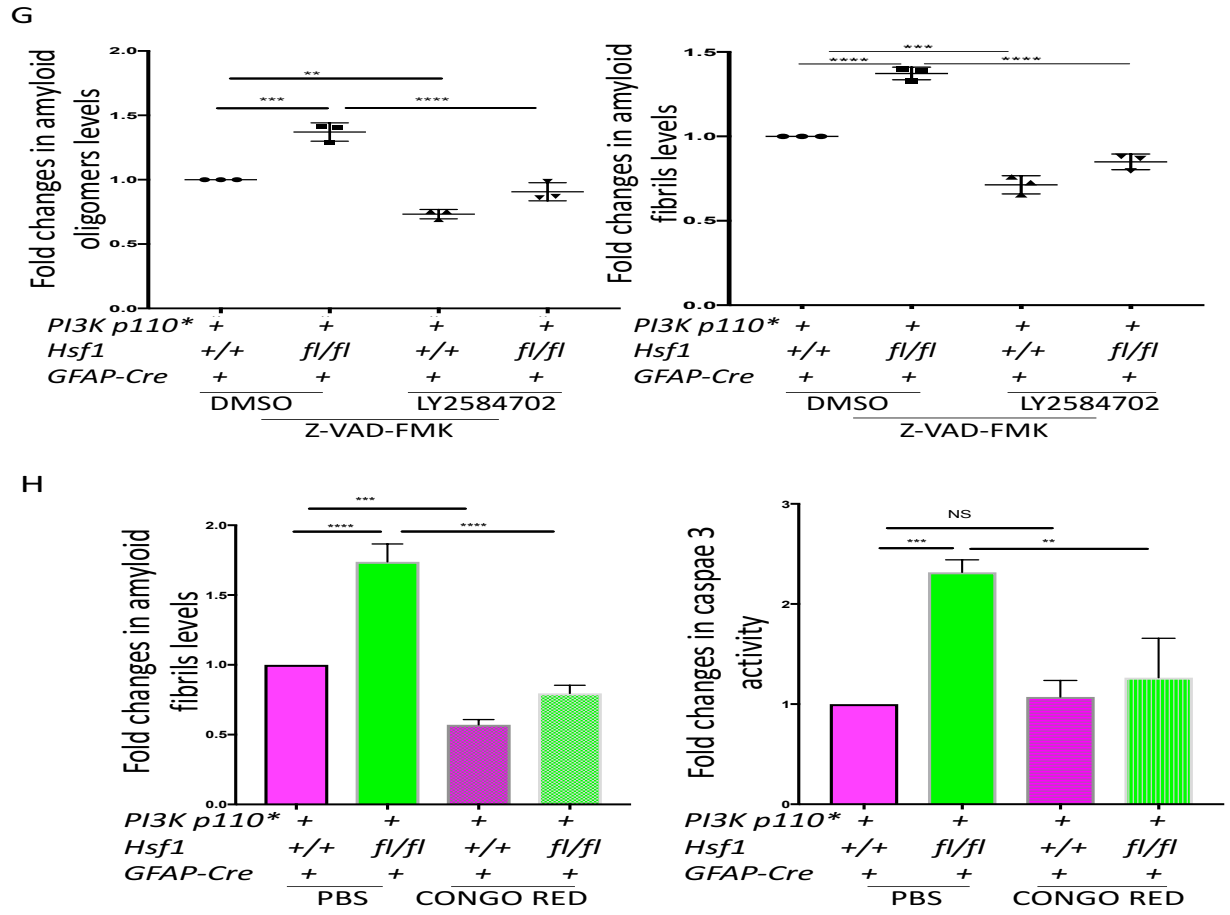

To test the key role of HSF1 activation by AKT in supporting tissue overgrowth, we deleted the tumor suppressor *Pten* to constitutively activate PI3K/AKT signaling. $Pten^{flox}$ mice possess *loxP* sites flanking exon 5 of the *Pten* gene. When used in conjunction with a Cre-expressing strain, *Pten* gene is deleted and PI3k/AKT signaling is constitutively activated (Fig 6 C) (Lesche, Groszer et al., 2002). We crossed $Pten^{fl/fl}$ mice with $Hsf1^{fl/fl}$ mice and *Albumin-Cre* mice to produce $Pten^{fl/fl};Hsf1^{+/+};Cre^{+}$, $Pten^{+/+};Hsf1^{fl/fl};Cre^{+}$, $Pten^{fl/fl};Hsf1^{fl/fl};Cre^{+}$, and $Pten^{+/+};Hsf1^{+/+};Cre+$ genotypes. The Cre recombinase is actively expressed in hepatocytes (Lee, Magnuson et al., 2003). So, PI3K/AKT signaling is constitutively activated in hepatocytes. $Pten^{+/+};Hsf1^{+/+};Cre^{+}$ mice serve as the controls (Fig 6 D). $Pten^{fl/fl};Hsf1^{fl/fl};Cre^{+}$ and $Pten^{fl/fl};Hsf1^{+/+};Cre^{+}$ mice were tested for the effects of *Hsf1* on liver overgrowth in *Pten* deleted background. All $Pten^{fl/fl};Hsf1^{+/+};Cre^{+}$ mice had enlarged livers compared to the control group (Fig 6 D). In contrast, $Pten^{fl/fl}$ mice with homozygous *Hsf1* deletion showed significantly reduced liver size (Fig 6 D). All these findings confirm that *Hsf1* knockout impairs the tissue overgrowth driven by constitutively active PI3K/AKT signaling. Since HSF1 is a key player in maintaining proteome homeostasis, we wondered whether proteostasis maintained by HSF1 is required for the PI3K/AKT-driven overgrowth. In our model, on the one hand PI3K/AKT signaling increases protein quantity through mTOCR1; and on the

other hand, PI3K/AKT signaling activates HSF1 to maintain protein quality. We hypothesized that deletion of *Hsf1* would disrupt the balance between protein quantity and protein quality. To test this hypothesis, we first investigated whether proteome is imbalanced by detecting amyloid fibrils in the brains of *PI3K p110*$^{*+}$*;Hsf1*$^{+/+}$*;Cre*$^{+}$ mice. Amyloid fibrils are special protein aggregates with highly ordered β-sheet structures and are toxic to the cells. The process in which certain misfolded monomeric proteins first form intermediate soluble amyloid oligomers, which further assemble into insoluble amyloid fibrils, is called amyloidogenesis (Outeiro, 2011). High levels of amyloids indicate severe proteotoxic stress and result in cellular toxicity (Ancsin, 2003). We found that, amyloid fibrils were induced in the brains of both *PI3K p110*$^{*+}$*;Hsf1*$^{+/+}$*;Cre*$^{+}$ and *PI3K p110*$^{*+}$*;Hsf1*$^{fl/fl}$*;Cre*$^{+}$ mice, and that *PI3K p110*$^{*+}$*;Hsf1*$^{fl/fl}$*; Cre*$^{+}$ mice had the highest levels of amyloid fibrils (Fig 6 E). Remarkably, we detected elevated Caspase 3 activity only in the brains of *PI3K p110*$^{*+}$*;Hsf1*$^{fl/fl}$*;Cre*$^{+}$ mice mice, (Fig 6 F), which indicates that HSF1 suppresses the toxicity caused by amyloidogenesis. To test whether PI3K/AKT signaling induces amyloidogenesis by increasing protein translation, we used a potent p70S6K inhibitor, LY2584702, to block protein translation in the astrocytes from the *PI3K p110*$^{*+}$*;Hsf1*$^{fl/fl}$*;Cre*$^{+}$ and *PI3K p110*$^{*+}$*;Hsf1*$^{+/+}$*;Cre*$^{+}$ mice. LY2584702 inhibits S6K to reduce protein translation (Tolcher, Goldman et

al., 2014). Inhibition of translation reduced the levels of amyloid oligomers and amyloid fibrils in both astrocytes (Fig 6 G), which indicates that increased protein translation driven by PI3K/AKT signaling provokes amyloidogenesis. We used Congo Red, a fluorescence dye selectively binding to amyloid structures and preventing amyloid formation (Lorenzo and Yankner, 1994) (Girych, Gorbenko et al., 2016), to treat the astrocytes from *PI3K p110*$^{*+}$*;Hsf1*$^{fl/fl}$*;Cre*$^{+}$ and *PI3K p110*$^{*+}$*;Hsf1*$^{+/+}$*;Cre*$^{+}$ mice. We found decreased levels of amyloid fibrils in both groups, and most importantly, reduced caspase 3 activity (Fig 6 H). This result demonstrates a causative role of amyloidogenesis in cell death. All these results suggest that HSF1 promotes overgrowth driven by constitutively active PI3K/AKT signaling by preventing cell death induced by amyloidogenesis.

2.3.7 HSF1 suppresses Amyloidogenesis-induced Cell Death

How does HSF1 protect cells from the amyloidogenesis-induced toxicity? Since apoptosis is often triggered by mitochondrial damage, we wondered whether the astrocytes from *PI3K p110*$^{*+}$*;Hsf1*$^{fl/fl}$*;Cre*$^{+}$ mice had increased apoptosis due to mitochondrial damage. We observed elevated levels of poly-ubiquitinated proteins and decreased levels of the mitochondrial marker TOMM20 proteins, which indicate mitochondrial damage in these astrocytes (Fig 7 A). Also, the localization of HSP60, the key chaperone in the mitochondria, was significantly altered in these astrocytes. HSP60 showed diffused staining into both the cytoplasm and nuclei in the astrocytes from *PI3K p110*$^{*+}$*;Hsf1*$^{fl/fl}$*;Cre*$^{+}$ mice (Fig 7 A B). In addition, we found small foci of HSP60 in these astrocytes (Fig 7 B), which suggests HSP60 aggregation. To further verify HSP60 aggregation, we detected HSP60 levels in the detergent-soluble and -insoluble fractions of the mouse brain lysates.

Figure 7. HSF1 suppresses amyloidogenesis-induced cell death by preventing HSP60 from aggregating

(A) Mitochondria are damaged in *PI3K p110*$^{+}$;Hsf1$^{fl/fl}$;Cre^{+}* astrocytes. Proteins were detected by immunoblotting in astrocytes after both mitochondrial and cytoplasmic fractions were separated. Blotting confirmed that elevated levels of poly-ubiquitinated proteins and PARKIN proteins, decreased levels of TOMM20 proteins in the mitochondrial fractions and that HSP60 and cytochrome C translocated from the mitochondria to the cytoplasm. MITO: mitochondrial fraction. CYTO: cytoplasmic fraction.

(D) Loss of soluble HSP60 proteins is not due to transcriptional regulation. *Hsp60* mRNA levels in brains were quantitated by qRT-PCR (mean±SD, n=5 brains, one-way ANOVA). qRT-PCR confirmed that *Hsp60* mRNA level had no significant differences among four genotypic groups of mice.

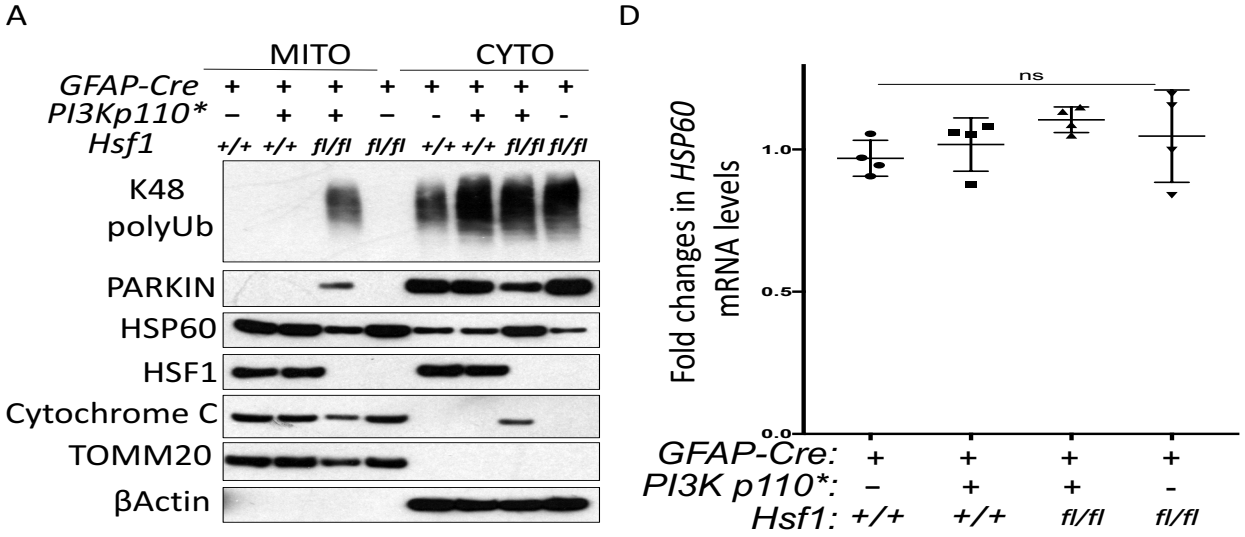

Figure 7 continued

(B) Hsf1 deficiency changes HSP60 localization pattern in PI3K p110*+;Hsf1fl/fl;Cre+ astrocytes. Astrocytes were stained with anti-HSP60 antibodies. Arrowheads mark HSP60 foci. IF staining confirmed that HSP60 diffused from the mitochondria into the cytoplasm in the astrocytes from PI3K p110*+;Hsf1fl/fl;Cre+ mice. Scale bar is 10μm.

(C) HSF1 prevents HSP60 aggregation in PI3K p110*-expressing mouse brains. Proteins were detected by immunoblotting in detergent-soluble and -insoluble fractions of mouse brain tissues. Blotting confirmed that TOMM20 levels were decreased in the brains of *PI3K p110*$^{*+}$*;Hsf1*$^{fl/fl}$*;Cre*$^{+}$ mice compared to the other groups, and HSP60 levels were decreased in the detergent-soluble fractions and increased in the detergent-insoluble fractions of the brain tissues of *PI3K p110*$^{*+}$*;Hsf1*$^{fl/fl}$*;Cre*$^{+}$ mice. SOLUBLE: soluble fraction. INSOLUBLE: insoluble fraction.

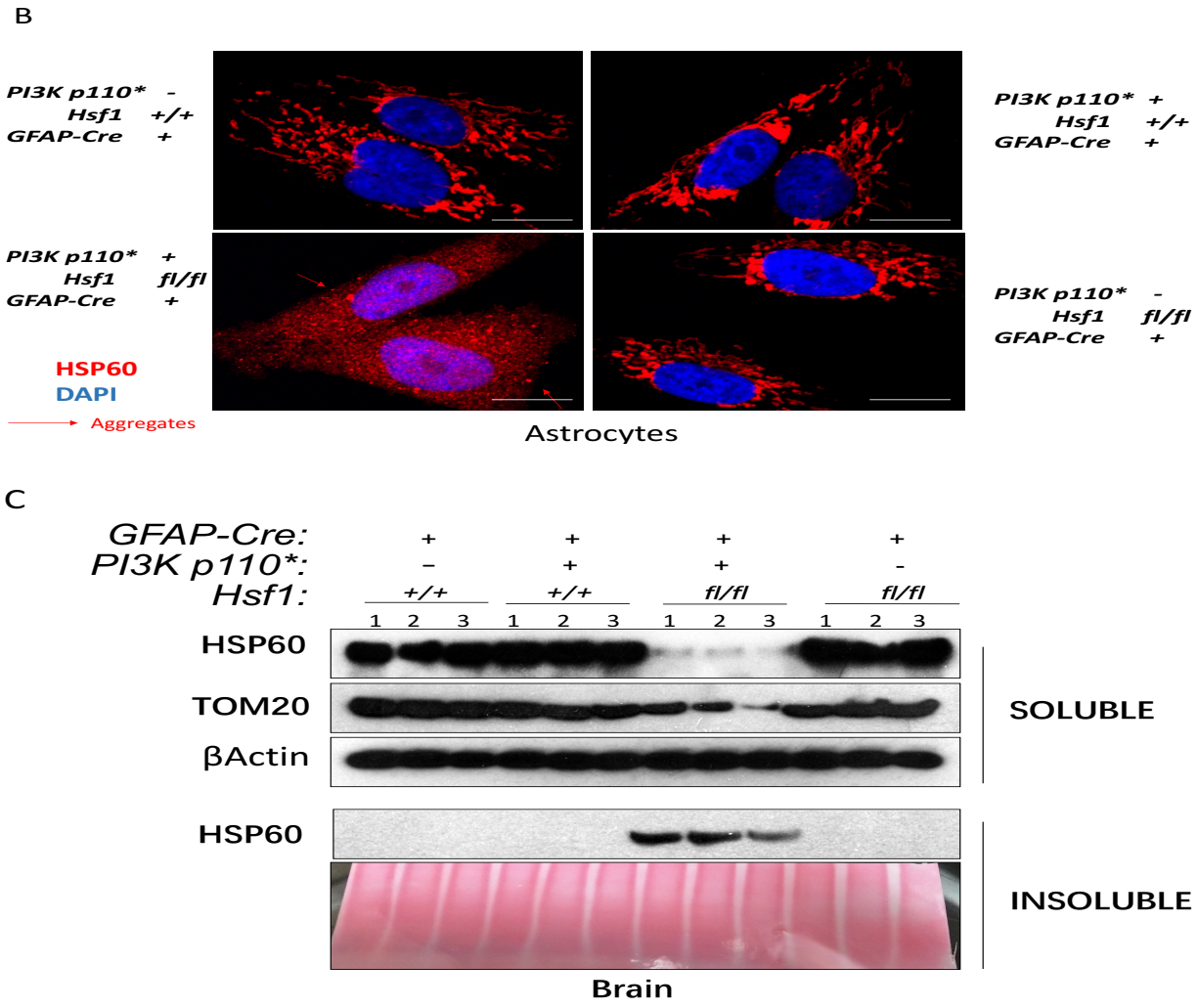

Figure 7 continued

(E) Loss of HSP60 causes mitochondrial damage. Proteins were detected by immunoblotting in astrocytes transfected with siRNAs targeting *Hsp60* after the mitochondrial and cytoplasmic fractions were separated. Blotting confirmed that knocking down *Hsp60* in *PI3K p110*$^{+}$;Hsf1$^{+/+}$;Cre^{+}* astrocytes elevated poly-ubiquitinated proteins and PARKIN and decreased TOMM20 proteins in the mitochondrial fractions, and caused HSP60 and cytochrome C to translocte from the mitochondria to the cytoplasm. MITO: mitochondrial fraction. CYTO: cytoplasmic fraction.

(F) Loss of HSP60 causes apoptosis. Caspase 3 activities were detected in astrocytes transfected with siRNAs targeting *Hsp60*. Caspase 3 activities confirmed that knocking down *Hsp60* in *p110*$^{+}$;Hsf1$^{+/+}$;Cre^{+}* astrocytes induced cell death.

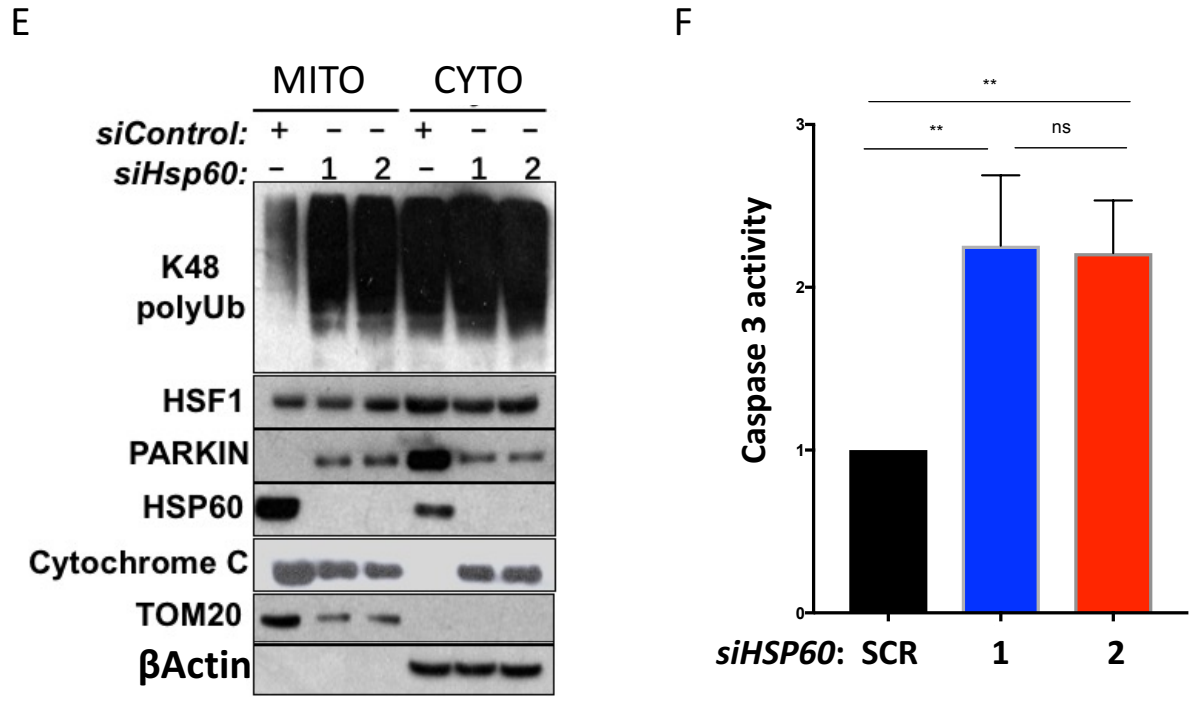

Figure 7 continued

(G) Amyloid oligomer (AO) physically interacts with HSP60. Endogenous AO-HSP60 interactions were detected by PLA in astrocytes using a rabbit anti-AO antibody and a mouse anti-HSP60 antibody. PLA staining confirmed that there is a physical association between AO and HSP60 only in *PI3K p110*$^{*+}$*;Hsf1*$^{fl/fl}$*;Cre*$^{+}$ astrocytes. Scale bar is 10μm.

(H) Amyloid oligomer (AO) physically interacts with HSP60. Endogenous HSP60 proteins were precipitated from brain lysates using the specific anti-AO antibody. WCL: whole cell lysate. Blotting confirmed that there is a physical association between AOs and HSP60 only in *PI3K p110*$^{*+}$*;Hsf1*$^{fl/fl}$*;Cre*$^{+}$ brains.

G

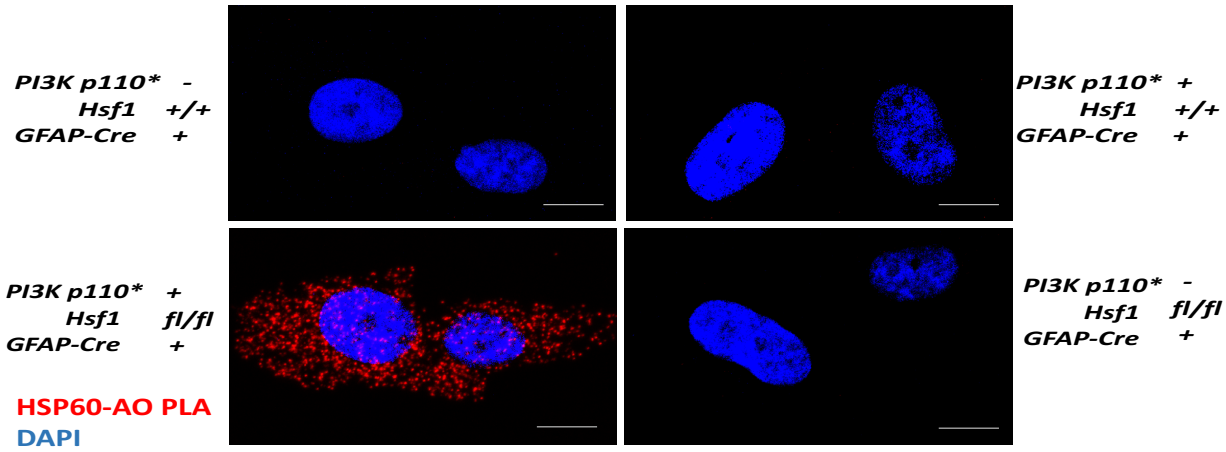

H

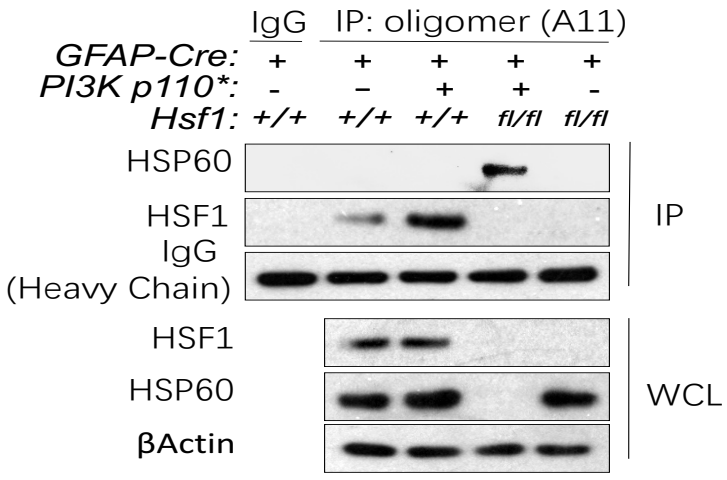

Figure 7 continued

(I) Overexpression of HSP60 rescues mitochondrial damage in *PI3K p110*$^{*+}$*;Hsf1*$^{fl/fl}$*;Cre*$^{+}$ astrocytes. Proteins were detected by immunoblotting in astrocytes transduced with lentiviral LACZ or HSP60 after the mitochondrial and cytoplasmic fractions were separated. Blotting confirmed that overexpression of HSP60 decreased poly-ubiquitinated proteins and PARKIN but increased TOMM20 proteins in the mitochondrial fraction, and prevented HSP60 and cytochrome C from translocating to the cytoplasm. MITO: mitochondrial fraction. CYTO: cytoplasmic fraction.

(J) Overexpression of HSP60 rescues cell death in *PI3K p110*$^{*+}$*;Hsf1*$^{fl/fl}$*;Cre*$^{+}$ astrocytes. Caspase 3 activities were detected in astrocytes transduced with lentiviral LACZ or HSP60. Caspase 3 activities confirmed that overexpression of HSP60 in *PI3K p110*$^{*+}$*;Hsf1*$^{fl/fl}$*;Cre*$^{+}$ astrocytes prevented cell death.

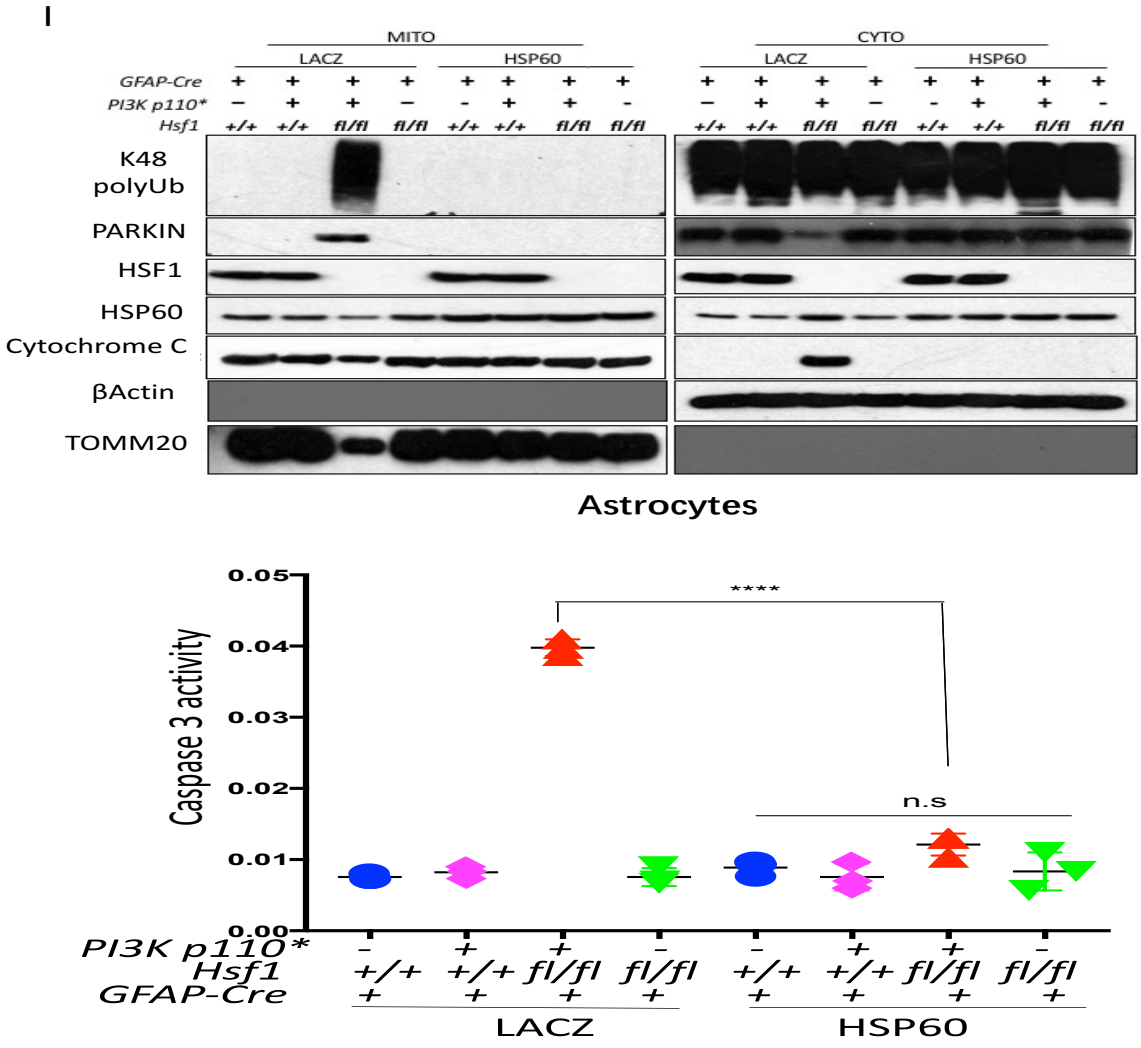

Figure 7 continued

(K) HSF1 prevents the HSP60-AO interactions. Endogenous AO-Hsp60 interactions and AO-HSF1 interactions were detected by PLA in astrocytes using a rabbit anti-AO antibody (A11), a mouse anti-HSP60 antibody and a mouse anti-HSF1 antibody. PLA staining confirmed that $HSF1^{WT}$ and N-terminus mutants ($HSF1^{1-379}$), but not C- terminus mutants ($HSF1^{380-529}$), blocked the interaction between HSP60 and AOs, and $HSF1^{WT}$ and N-terminus mutants ($HSF1^{1-379}$), but not C- terminus mutants ($HSF1^{380-529}$), directly interacted with AOs. Scale bar is 10μm.

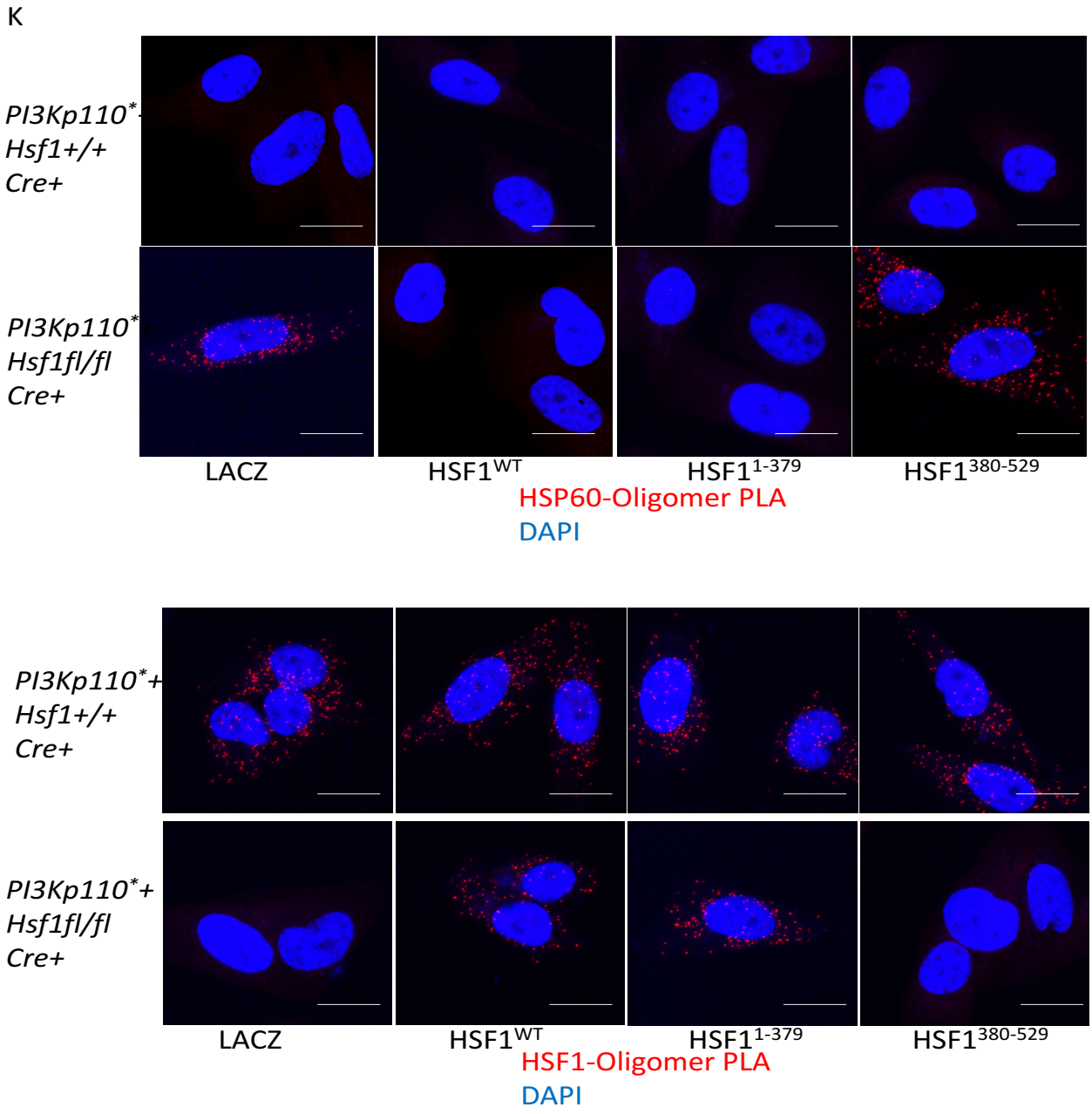

Figure 7 continued

(L) HSF1 prevents HSP60 aggregation induced by Aβ amyloids *in vitro*. Recombinant human HSP60 proteins were incubated with $A\beta_{1\text{-}42}$ or 42-1 $A\beta_{42\text{-}1}$ peptides in the presence of recombinant GST or human His-HSF1 proteins. Following shaking at 37^0C for 72 hours and centrifugation, proteins were detected by immunoblotting in the supernatants and pellets. Blotting confirmed that HSP60 aggregation caused by $A\beta_{1\text{-}42}$ peptides was blocked by recombinant HSF1 proteins.

(M) Schematic description of the protection of mitochondria from amyloids by HSF1. Under proteotoxic stress conditions, in *Hsf1*-proficient cells amyloid oligomers interact with HSF1, instead of HSP60, in the mitochondria; so HSP60 can function as a major chaperone to maintain mitochondrial proteome homeostasis. However, in *Hsf1*-deficient cells, amyloid oligomers directly attack HSP60 in the mitochondria to cause its aggregation, leading to misfolding and aggregation of other mitochondrial proteins, which finally induces mitochondrial damage and apoptosis.

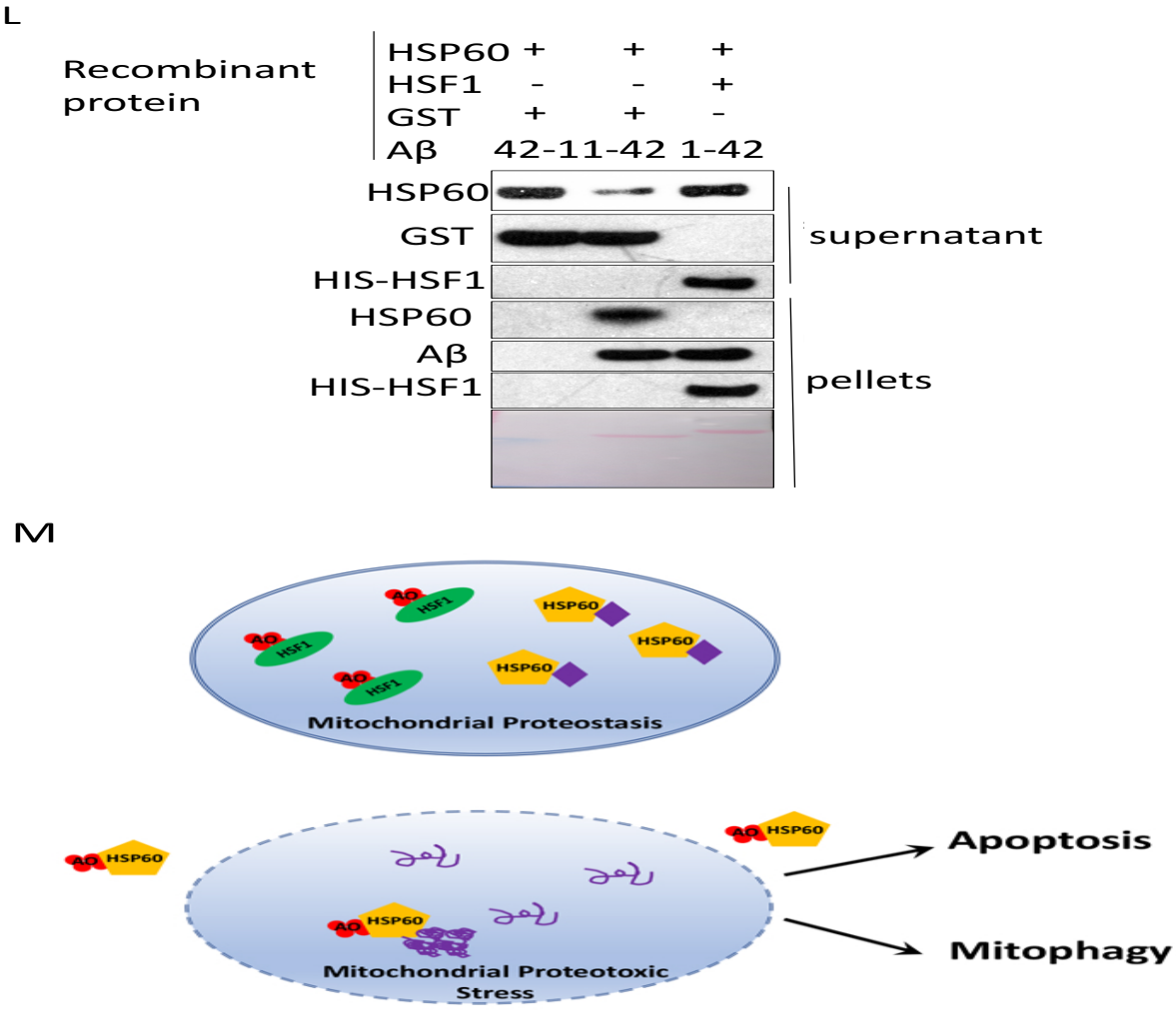

Consistent with the finding in astrocytes, TOMM20 levels were decreased in the brain tissues of *PI3K p110^{*+};Hsf1$^{fl/fl}$;Cre^{+}* mice compared to the other groups (Fig 7 C), which confirmed mitochondrial damage. Strikingly, HSP60 levels decreased in the soluble fractions but increased in the insoluble fractions of the brain tissues of *PI3K p110^{*+};Hsf1$^{fl/fl}$;Cre^{+}* mice (Fig 7 C), although no significant changes were detected in *Hsp60* mRNA levels (Fig 7 D). These results indicate that loss of HSP60 proteins in the brains of *PI3K p110^{*+};Hsf1$^{fl/fl}$;Cre^{+}* mice was due to HSP60 aggregation. Knockdown of *Hsp60* in the *PI3K p110^{*-};Hsf1$^{+/+}$;Cre^{+}* astrocytes mimicked the phenotypes of the *PI3K p110^{*+};Hsf1$^{fl/fl}$;Cre^{+}* astrocytes, which resulted in increased poly-ubiquitinated proteins and decreased TOMM20 proteins in the mitochondria, translocation of HSP60 from the mitochondria to the cytoplasm, and elevated Caspase 3 activities (Fig 7 E F). In addition, restoration of HSP60 levels in the *PI3K p110^{*+};Hsf1$^{fl/fl}$;Cre^{+}* astrocytes rescued mitochondrial damage and cell death, indicated by reduced poly-ubiquitinated proteins and increased TOMM20 proteins in the mitochondria, and reduced caspase 3 activities (Fig 7 I J). These results establish the causative role of HSP60 loss in mitochondrial damage and cell death. To further dissect how HSP60 aggregation is induced, we investigated the possibility that amyloid oligomers (AOs) directly interacts with HSP60 proteins using both PLA and CoIP. HSP60 directly binds to AOs in the

astrocytes and brain tissues from *PI3K p110*$^{*+}$*;Hsf1*$^{fl/fl}$*;Cre*$^{+}$ mice (Fig 7 G H). These results suggest that HSF1 protects HSP60 from interacting with AOs. Next, we investigated how HSF1 prevents HSP60 aggregation by over-expressing HSF1 wide-type (HSF1^{WT}), HSF1 N-terminus mutants (HSF1$^{1-379}$), which lack the transactivation domain, and HSF1 C-terminus mutants (HSF1$^{380-529}$), which lack the DNA binding domain, in both *PI3K p110*$^{*+}$*;Hsf1*$^{fl/fl}$*;Cre*$^{+}$ and *PI3K p110*$^{*+}$*;Hsf1*$^{+/+}$*;Cre*$^{+}$ astrocytes. Expression of HSF1 wide-type (HSF1^{WT}) and N-terminus mutants (HSF1$^{1-379}$), but not C-terminus mutants (HSF1$^{380-529}$), in the *PI3K p110*$^{*+}$*;Hsf1*$^{fl/fl}$*;Cre*$^{+}$ astrocytes blocked the interactions between HSP60 and AOs (Fig 7 K). Importantly, HSF1 wide-type (HSF1^{WT}) and N-terminus mutants (HSF1$^{1-379}$) directly interacted with AOs, instead of HSP60 (Fig 7 K). These results strongly suggest that HSF1 protects HSP60 from aggregation through physical interactions. In addition, recombinant HSF1 proteins prevented the aggregation of recombinant HSP60 proteins induced by $A\beta_{1-42}$ amyloid peptides *in vitro* (Fig 7 L). So, our results indicate that HSF1 protects cell from the amyloidogenesis-induced toxicity by preventing HSP60 aggregation and maintaining the mitochondrial proteome homeostasis (Fig 7 M).

2.4 Discussion

2.4.1 HSF1 is a New Physiological Substrate of AKT

Our studies now show that AKT directly phosphorylates HSF1 at Ser230 site. Previously, we discovered that the oncoprotein MEK directly phosphorylates HSF1 at Ser326 site. Although both phosphorylation events activate HSF1, the underlying mechanisms are different. While the MEK-mediated Ser326 phosphorylation promotes HSF1 nuclear translocation and DNA binding, the AKT-mediated Ser230 phosphorylation does not affect this process and only enhances its DNA binding. These distinct effects are consistent with the observation that both phosphorylation events are independent of each other and activate HSF1 in an additive manner. Our findings also suggest HSF1 could be activated through phosphorylation by separate oncogenic pathways in different tumors. However, whether other oncogenic signaling can regulate HSF1 through other mechanism, such as nuclear translocation and trimerization, is still a big question worth to explore in the future.

2.4.2 AKT drives Growth by coordinating Protein Quantity- and Quality-control Machineries

As a key player in growth control, AKT appears to govern two discrete but well-coordinated downstream effector pathways, of which one is mediated by HSF1 to control protein quality and the other by mTORC1 to control protein quantity. On the one hand, constitutively active PI3K/AKT signaling provokes proteomic chaos by markedly increasing protein quantity through mTORC1, and on the other hand, through HSF1 activation, PI3K/AKT signaling heightens cellular chaperoning capacity to ensure productive protein synthesis. Balanced protein quantity and quality leads to proteostasis and robust growth. This is supported by our observation that deletion of *Hsf1* disrupts proteostasis and impairs tissue overgrowth driven by constitutive activation of PI3K/AKT signaling. Interestingly, our study is the first one to report constitutively active PI3K/AKT signaling can maintain proteome homeostasis through activating HSF1. However, there are many other effectors mediating proteome homeostasis, such as proteasome pathways, autophagy pathways and unfolded protein response (UPR) pathways. So, it will be exciting to investigate whether constitutively active PI3K/AKT signaling can regulate any of these pathways to maintain proteome homeostasis in the future.

2.4.3 Guarding of Mitochondrial Proteostasis by HSF1 through Prevention of HSP60 Aggregation

Our findings uncover a new role of HSF1 in regulating mitochondrial proteostasis to promote overgrowth, which is independent of its transcriptional function. One of the key consequences of disruption of proteostasis is the emergence of amyloids. It has been widely recognized that amyloids are toxic to the cells, particularly neurons. Although many mechanisms by which amyloids induce neurotoxicity have been proposed, the precise direct molecular targets of amyloids underlying neurotoxicity has remained controversial. Our data supports that soluble amyloid oligomers are the primary inducer of cellular toxicity. In addition, our study provides a new theory of how soluble amyloid oligomers induce cellular toxicity. In the absence of HSF1, amyloid oligomers directly induce aggregation of HSP60, which ultimately leads to mitochondrial damage and cell death. We also think that this could be the same mechanism of how amyloidogenesis induce tumor cells death when HSF1 is diminished and proteome homeostasis is disrupted in tumors. Furthermore, we unveiled that HSF1 can suppress amyloid formation through physical interaction, which has a great therapeutic potential to treat amyloid diseases in humans in the future.

2.5 Experimental Procedures

2.5.1 Cells and Tissues

HEK293T, HeLa, A2058 cells were purchased from ATCC. Primary astrocytes were directly derived from neonatal mouse brains. All cells were cultured in DMEM supplemented with 10% fetal bovine serum. Brain and liver tissues were directly derived from mice and stored in -80^{o}C.

2.5.2 Proximity Ligation Assay

Cells were fixed with 4% formaldehyde in PBS for 15 minutes at room temperature and blocked with 5% normal goat serum in PBS with 0.3% Triton X-100. Primary antibodies were 1:100 diluted in blocking buffer and used to incubate fixed cells overnight at 4°C. After incubation with Duolink PLA anti-rabbit Plus and anti-mouse Minus probes (1:5, OLINK Bioscience) at 37°C for 1 hour, ligation for 0.5 hour and amplification for 110 minutes, Nuclei were stained with Hoechst 33342. Then PLA signals were documented by a Zeiss 780 confocal microscope or quantified by flow cytometry.

2.5.3 Real-time Quantitative RT–PCR

Total RNAs were extracted using RNA STAT-60 reagent (Tel-Test), and RNAs were reverse transcripted using a High Capacity Reverse Transcription kit (Applied Biosystems). Equal amounts of cDNAs were

used for quantitative RCR reaction using a DyNAmo SYBR Green qPCR kit (Thermo Scientific). Signals were detected by an ABI 7500 Real-Time PCR System (Applied Biosystems) and Stratagene Mx3000P real-time PCR System (Applied Biosystems). ACTB and 18S were used as the internal control.

2.5.4 Transfection and Luciferase Reporter Assay

TurboFect transfection reagent (Thermo Scientific) was used to transfect plasmids. The Ziva Ultra SEAP Plus Detection Kit (Jaden BioScience) was used to detect SEAP activities in culture supernatants while the Gaussia Luciferase Glow Assay Kit (Thermo Scientific) was used to detect Guassia luciferase activities. VICTOR3 Multilabel plate reader (PerkinElmer) was used to measure the luminescence.

2.5.5 Cell Apoptosis Assay

A caspase 3 DEVD-R110 Fluorometric and Colorimetric Assay kit (Biotium) was used to detect caspase 3 activity.

2.5.6 Measurement of Liver Cell Size

Mouse liver cells were mechanically dissociated in PBS containing 10% FBS. Livers were squeezed through a 70mm nylon cell strainers by a syringe head. After collecting single-cell suspensions by

centrifuging at 500g for 5 min, cells were washed three times with PBS–FBS and analyzed by flow cytometry. The primary cell populations were gated for size measurement based on forward scatter.

2.5.7 shRNA and siRNA Knockdown

Lentiviral pLKO shRNA plasmids targeting human PTEN were obtained from Addgene. MISSION siRNAs: HSPD1 were purchased from Sigma-Aldrich. The non-targeting siRNA control (D-001810-01) was purchased from Dharmacon GE Healthcare.

2.5.8 *In vitro* Kinase Assay

100 ng HSF1 proteins were incubated with 30µl kinase buffer (25mM MOPS pH 7.2, 12.5mM β-glycerol-phosphate, 25mM MgCl2, 5mM EGTA, 2mM EDTA, 0.25mM dithiothreitol, 250µM ATP) and 100 ng recombinant GST, AKT1, AKT2, AKT3, MEK1, CaMKII or DAPK active proteins (SignalChem) at 30°C for 30 minutes with 1,200 r.p.m. mixing in an Eppendorf ThermoMixer. Reactions were stopped by adding 20µl 2× sample buffer with 3% 2-mercaptoethanol.

2.5.9 Animal Studies

R26Stop^{FL}P110* (PI3K p110*) mice, *Hsf1$^{fl/fl}$* mice, *hGFAP-Cre* mice, *Pten$^{fl/fl}$* mice and *Albumin-Cre* mice on the C57BL/6 background were obtained from The Jackson Laboratory. *R26Stop^{FL}P110* (PI3K p110*)*

mice were crossed with *Hsf1*$^{fl/fl}$ mice and *hGFAP-Cre* mice to produce *PI3K p110*$^{*+}$*;Hsf1*$^{fl/fl}$*;Cre*$^{+}$*, PI3K p110*$^{*+}$*;Hsf1*$^{+/+}$*; Cre*$^{+}$*, PI3K p110*$^{*-}$*;Hsf1*$^{fl/fl}$*;Cre*$^{+}$ and *PI3K p110*$^{*-}$*;Hsf1*$^{+/+}$*;Cre*$^{+}$ genotypes. *Pten*$^{fl/fl}$ mice were crossed with *Hsf1*$^{fl/fl}$ mice and *Albumin-Cre* mice to produce *Pten*$^{fl/fl}$*;Hsf1*$^{fl/fl}$*;Cre*$^{+}$*, Pten*$^{fl/fl}$*; Hsf1*$^{+/+}$*;Cre*$^{+}$*, Pten*$^{+/+}$*Hsf1*$^{fl/fl}$*; Cre*$^{+}$ and *Pten*$^{+/+}$*;Hsf1*$^{+/+}$*;Cre*$^{+}$ genotypes. Genotyping was performed by PCR using tail genomic DNAs. All mouse experiments were performed under protocol approved by both The Jackson Laboratory Animal Care and Use Committee and NCI Animal Care and Use Committee.

2.5.10 Immunofluorescence

Cultured cells were seeded on the slides and fixed with 4% formaldehyde for 15 minutes RT, then blocked with blocking buffer for 1 hour. 1:100 primary antibodies were applied to the slides and incubated at 4^0C overnight. 1:200 secondary antibodies were applied and incubated at RT for 1 hour. Fluorescent signals were captured by a Zeiss 780 confocal microscope and the images were analyzed with ImageJ software.

2.5.11 Detergent-soluble and -insoluble Fractionation

Equal numbers of cells were incubated with cell lysis buffer containing 1% Triton X-100 on ice for 20 minutes. The crude lysates were first centrifuged at 500 g for 5 min at 4°C. The supernatants were

collected as 1st supernatants. The pallets were digested with DNase I at RT for 20 minutes then further incubated with 50µl 2% SDS at RT for 30 minutes and centrifuged at max speed for 10 minutes at RT. The supernatants were collected as membrane fractions. Pellets were mixed with 1st supernatants and centrifuged at max speed at 4°C for 10 minutes. The supernatants were collected as soluble fractions and the pellets as insoluble fractions, which were further subjected to sonication for SDS–PAGE or ELISA.

2.5.12 Amyloid Oligomer and Fibril Quantitation by ELISA

Equal amount of proteins (20µg) from soluble fraction were incubated in each well of a 96 wells ELISA plate in a total volume of 100µl at 4^{0}C overnight. 100µl milk was used as blocking buffer to each wells and incubated at RT for 1 hour. 100µl milk containing oligomer antibodies (A11, 1:1000) was applied to each well at RT for 2 hours as primary antibody. Then 100µl milk containing secondary antibodies (rabbit, 1: 5000) was applied to each well and incubated at RT for 1 hour. 100µl 1-step Ultra TMB-ELISA was used as detection reagent. The ELISA signals were finally captured by spectraMAX 190. After quantification of proteins from insoluble fractions, equal amount of proteins was added to each well a 96 wells ELISA plate in a total volume of 100µl and incubated at 37°C without cover overnight to dry

the wells. The following steps were the same as the detection of amyloid oligomer except that primary antibodies for amyloid fibril are amyloid fibril antibodies (OC).

2.5.13 Statistics Analysis

Prism 6.0 (GraphPad software) was used to analyze the results. Two groups were compared by Unpaired two-tailed Student's t-test. Multiple groups were compared by one-way or two-way ANOVA. All samples and animals were included in the analyses.

CHAPTER 3

CONCLUSION AND FUTURE WORK

3.1 HSF1 is a New Physiological Target of AKT Kinase

PI3K/AKT signaling cascade is essential to cell growth and differentiation. Activated by growth factors, PI3K phosphorylates PIP2 to PIP3, which further phosphorylates PDK1. PDK1 phosphorylating AKT at T308 site at the cellular membrane leads to AKT partial activation. AKT is fully activated by mTORC2 through phosphorylation of S473 site (Guo, Tian et al., 2017). Upon activation, AKT can enter the nucleus to phosphorylate many downstream targets. Hundreds of proteins have been identified as AKT targets including TSC2, FoxO proteins and GSK3. AKT activates mTOCR1 through phosphorylating and inhibiting TSC2, which enables cell growth (Makker, Goel et al., 2014). In addition, AKT phosphorylates FoxO proteins, leading FoxO proteins out of the nucleus, which suppresses FoxO transcriptional program involved in the induction of apoptosis, cell cycle arrest, catabolism and growth inhibition (Atfi, Abecassis et al., 2005). Also, AKT is part of the growth factor signaling that mediates GSK3 phosphorylation (Hermida, Dinesh Kumar et al., 2017). Thus, AKT functions as a critical mediator for cell growth and survival through multiple interconnected pathways.

In our current study, we, for the first time, identified HSF1 as a target of AKT. Through *in vivo* and *in vitro* experiments, we found that AKT phosphorylates HSF1 at S230 site, which is an important modification during HSF1 activation. Phosphorylation of HSF1 S230 site is necessary to promote HSF1 activation. According to our results, HSF1 S230A mutants still exhibited certain levels of transcriptional activity and can be further activated by another oncoprotein MEK, which indicates that multiple signaling pathways regulate HSF1 activation through distinct phosphorylation sites independently. So far, we have discovered that HSF1 activity is regulated by tumor-suppressive AMPK signaling, oncogenic RAS/MEK and PI3K/AKT signaling. These findings suggest that HSF1 could be constitutively activated through distinct mechanisms in different tumors, depending on which mutations are present. Furthermore, there could be other oncogenic or tumor-suppressive pathways regulating HSF1, which is worth exploring in the future.

In this study, we found that Ser230 phosphorylation by AKT promotes HSF1 DNA binding but not its nuclear translocation. Regarding the process of HSF1 activation, however, there is an interesting question we have not answered in this project. Does this phosphorylation affect HSF1 trimerization? HSF1

trimerization is an indispensable step for its activation. However, the pathways regulating this step still remain elusive. So far, one study suggests that HSF1 trimerization is temperature-inducible (Hentze, Le Breton et al., 2016). It will be interesting to investigate in the future whether HSF1 is prone to forming trimers in tumor cells or whether HSF1 trimerization is promoted by oncogenic pathways such as PI3K/AKT or RAS/MEK signaling.

Constitutively activated PI3K/AKT signaling mobilizes HSF1 to guard against proteotoxic stress induced by protein overproduction driven by hyper-activated mTORC1. In our study, AKT governs both protein quantity- and quality-control machineries through mTOCR1 and HSF1, respectively. While it has been known that AKT regulates cell growth through many interconnected pathways such as mTOCR1, FoxO proteins and GSK3, it is discovered for the first time that AKT is directly involved in regulating proteomic quality. As mentioned before, proteotstasis is regulated by a network of pathways. So, we wonder whether PI3K/AKT pathway can protect proteostasis through other pathways besides HSF1. It was noted that PI3K/AKT signaling is activated during endoplasmic reticulum (ER) stress caused by accumulation of misfolded proteins inside ER. Thus, it would be interesting to investigate whether

PI3K/AKT signaling can activate the unfolded protein response (UPR), a key mechanism that fights against ER stress particularly, in the future.

3.2 A Mouse Model for Human Megalencephaly

Loss of *PTEN* through somatic mutations have been found in many human cancers (Gu, Ou et al., 2016) (Alimonti, 2010). Furthermore, activating mutations of PI3K and AKT have also been identified in human tumors (Samuels and Waldman, 2010) (Karakas, Bachman et al., 2006) (Yi and Lauring, 2016). Thus, hyper-activated PI3K/AKT signaling is considered as an attractive anti-cancer therapeutic target (Pal and Mandal, 2012) (Zhang, Jin et al., 2007). So far, many mouse models in which the PI3K/AKT signaling pathway is genetically modified have been generated to study tumorigenesis and tumor progression. For instance, $Pten^{+/-}$ mice develop tumors in multiple tissues, including the breast, endometrium and prostate, which demonstrate many features found in corresponding human cancers (Knobbe, Lapin et al., 2008). Transgenic mice carrying the *PI3KCA-H1047R* or *PI3KCA-E545K* mutation under the control of mammary gland-specific promoter developed breast cancer showing basal and luminal markers (Meyer, Koren et al., 2013). Expressing the *PI3KCA-H1*047R mutant in the lungs induced lung adenocarcinomas (Green, Trejo et al., 2015).

Although the PI3K/AKT signaling pathway is activated in 90% human glioblastomas, no mouse glioblastoma models carrying constitutively active *PI3KCA* or *AKT* mutations exist (Carnero and Paramio, 2014). So, in the beginning of our project, we set out to tackle this challenge, by activating PI3K/AKT signaling in neural progenitor cells, which can differentiate into both glia and neurons. Strikingly, instead of developing brain tumors, these mice showed enlarged brains and died within 20 days after birth. We suspected that these mice probably lived too short to develop tumors, which is probably due to the massive expression of *p110** in the brain. So, we propose alternative strategies to generate a glioblastoma mouse model by crossing $R26Stop^{FL}P110^{*}$ mice with $GFAP\text{-}CreER^{T2}$ mice. Then, we can deliver tamoxifen into the brains through intracranial injections. It is a promising strategy that has been used to generate mouse models of glioblastoma expressing other oncogenes previously (Lenting, Verhaak et al., 2017).

Although the mice in our study did not develop glioblastomas, they indeed displayed the phenotypes resembling human megalencephaly. Megalencephaly is a developmental disorder characterized by brain overgrowth. Recent genetic studies have revealed that megalencephaly in human is caused by activating mutations of the components of PI3K/AKT signaling (Riviere, Mirzaa et al., 2012). Patients of

megalencephaly have abnormally large brains that are 2.5 standard deviations above the general population (Mirzaa, Riviere et al., 2013). To our knowledge, our *hGFAP-Cre*; *R26Stop*^{FL}*P110** mice are the first mouse model of megalencephaly that recapitulates the same genetic alterations in humans. In addition, our mouse model can be used to test the potential treatments for this disease. In our current study, deletion of *Hsf1* reduced brain size and prolonged mice lifespan, which is due to increased cell death caused by severe proteotoxic stress. Interestingly, in our previous study, we showed that the combination of MEK and proteasome inhibition inactivated HSF1 in tumor cells, which leads to severe proteotoxic stress and cell death. Thus, we speculated that treatment of the megalencephaly mice with combined MEK and proteasome inhibitors may alleviate the symptoms and prolong their lifespans. Apparently, more work is needed to test our hypothesis in the future. Another important direction for our future work is to verify the key findings in the mouse models using patient tissues. We would like to get some brain tissues from both healthy people and patients with megalencephaly. We are very interested in investigating whether disruption of proteostaiss, evidenced by elevated protein polyubiqitination and amyloidogenesis, and HSF1 activation are associated with human megalencephaly.

3.3 HSF1 suppresses Amyloidogenesis through Physical Interaction

Amyloidogenesis is a process in which specific proteins converse from their native soluble functional states into highly ordered filamentous amyloid fibrils (Tycko, 2014). Amyloidogenesis is associated with a number of neurodegenerative disorders. In each of these pathological conditions, a particular protein first convert from its native, functional state into small intermediates – soluble amyloid oligomers, and further into insoluble amyloid fibrils with enriched β-sheet structures (Tofoleanu and Buchete, 2012). Interestingly, amyloid oligomers or amyloid fibrils formed by proteins or peptides with discrete amino acid sequences share a common conformation that can be recognized specifically by antibodies (Kayed, Head et al., 2007). So far, more than 20 proteins, that can form amyloid oligomers and amyloid fibrils under certain human pathological conditions, have been identified (Chiti and Dobson, 2017). In our study, we found that in the mouse model of megalencephaly, amyloidogenesis is elevated in the overgrown brains. We further showed that PI3K/AKT signaling induced amyloidogenesis by enhancing the mTORC1-meditaed protein translation. In contrast, amyloidogenesis has not been associated with megalencephaly and the identifications of these amyloids remain unknown. Thus, in the future work, we will address this question using the brain samples from both our mouse models and human

megalencephaly patients. Following immunoprecipitating amyloid oligomers using the amyloid conformation-specific antibody A11, the potential amyloids can be identified by mass spectrometry. Clearly, amyloidogenesis can lead to cell death. However, whether soluble amyloid oligomers or insoluble amyloid fibrils are the primary inducer of cellular toxicity remains uncertain. Early research focusing on Alzheimer's disease suggested that large amyloid fibrils cause neuronal cell death and disease pathology. However, over the years, researchers found that in Alzheimer's disease, there was no correlation between Aβ amyloid fibrils deposition and the severity of this disease (Ow and Dunstan, 2014). Instead, the levels of soluble Aβ oligomers in the brains of patients of Alzheimer's disease were found to be correlated with cognitive impairment in several studies (Hayden and Teplow, 2013) (Benilova, Karran et al., 2012) (Viola and Klein, 2015). Furthermore, in the case of Parkinson disease, injection of α-synuclein oligomers, but not α-synuclein fibrils, caused neuronal cell death (Winner, Jappelli et al., 2011). These findings together suggest that soluble amyloid oligomers are the real culprit leading to cellular toxicity. To date, two mechanisms have been proposed for how soluble amyloid oligomers induce cellular toxicity. One group suggested that Aβ oligomers damage the lipid bilayer of the cellular membrane by affecting phospholipid composition and negative charges (Canale, Seghezza et al.,

2013). The other study pointed out that amyloid oligomers ubiquitously elevated intracellular Ca^{2+} levels, which leads to toxicity and elicits downstream pathological events (Demuro, Mina et al., 2005) (Mattson, Cheng et al., 1992). In contrast, our study unveiled an entirely new model. In the absence of HSF1, amyloid oligomers directly induce aggregation of HSP60, an essential mitochondrial chaperone, which causes disruption of mitochondrial proteostasis that ultimately leads to mitochondrial damage and cell death. In our previous study, we demonstrated that amyloidogenesis caused by the combination of MEK and proteasome inhibitors induce apoptosis in tumor cells. However, we had not elucidated the mechanisms at that time. According to our new findings, we hypothesize that it may be the same mechanism we uncovered in the overgrown brains. To test this, in future work, we plan to study whether amyloid oligomers binds to HSP60 after combined treatment of MEK and proteasome inhibitors in tumor cells.

Of note, there is no approved therapeutic reagents to target amyloids although several designed peptides and small polyphenol molecules have been demonstrated to inhibit the assembly of amyloid fibrils (Porat, Abramowitz et al., 2006) (Martins, 2013) (Zraika, Aston-Mourney et al., 2010). In our study, we discovered for the first time that a transcription factor – HSF1 – can directly interact with amyloid

oligomers and markedly suppress the formation of amyloid fibrils. Importantly, HSF1 blocks amyloidogenesis independent of its transcription activity. In addition to guarding proteostasis by upregulating the expression of molecular chaperones, HSF1 directly binds to amyloid oligomers, which not only prevents amyloid oligomers assembling into amyloid fibrils but also protects other essential proteins such as HSP60 from the direct attack by amyloids. This novel function of HSF1 has not been discovered previously. Our studies suggest that HSF1 could be exploited to treat amyloid diseases such as Alzheimer's disease, Parkinson's disease, Huntington's disease and amyotrophic lateral sclerosis (ALS). While much effort has been focused on identifying HSF1 activators, which can improve proteostasis by inducing the transcription of *HSPs*, the anti-amyloid effect of HSF1 through physical interactions has not been exploited. In another ongoing project of ours, we screened a HSF1 peptide library and found that several HSF1 peptides are able to block the assembly of amyloid fibrils. Thus, these peptides may have a great therapeutic potential to treat amyloid diseases in humans.

REFERENCES

Akerfelt, M., R. I. Morimoto and L. Sistonen. Heat shock factors: integrators of cell stress, development and lifespan. Nat Rev Mol Cell Biol. 2010. 11:545-555.

Alimonti, A. PTEN breast cancer susceptibility: a matter of dose. Ecancermedicalscience. 2010. 4:192.

Anckar, J. and L. Sistonen. Regulation of HSF1 function in the heat stress response: implications in aging and disease. Annu Rev Biochem. 2011. 80:1089-1115.

Ancsin, J. B. Amyloidogenesis: historical and modern observations point to heparan sulfate proteoglycans as a major culprit. Amyloid. 2003. 10:67-79.

Atfi, A., L. Abecassis and M. F. Bourgeade. Bcr-Abl activates the AKT/Fox O3 signalling pathway to restrict transforming growth factor-beta-mediated cytostatic signals. EMBO Rep. 2005. 6:985-991.

Batulan, Z., G. A. Shinder, S. Minotti, B. P. He, M. M. Doroudchi, J. Nalbantoglu, M. J. Strong and H. D. Durham. High threshold for induction of the stress response in motor neurons is associated with failure to activate HSF1. J Neurosci. 2003. 23:5789-5798.

Benderska, N., J. Ivanovska, T. T. Rau, J. Schulze-Luehrmann, S. Mohan, S. Chakilam, M. Gandesiri, E. Ziesche, T. Fischer, S. Soder, A. Agaimy, L. Distel, H. Sticht, V. Mahadevan and R. Schneider-Stock. DAPK-HSF1 interaction as a positive-feedback mechanism stimulating TNF-induced apoptosis in colorectal cancer cells. J Cell Sci. 2014. 127:5273-5287.

Benilova, I., E. Karran and B. De Strooper. The toxic Abeta oligomer and Alzheimer's disease: an emperor in need of clothes. Nat Neurosci. 2012. 15:349-357.

Bett, J. S. Proteostasis regulation by the ubiquitin system. Essays Biochem. 2016. 60:143-151.

Blake, J. F., R. Xu, J. R. Bencsik, D. Xiao, N. C. Kallan, S. Schlachter, I. S. Mitchell, K. L. Spencer, A. L. Banka, E. M. Wallace, S. L. Gloor, M. Martinson, R. D. Woessner, G. P. Vigers, B. J. Brandhuber, J. Liang,

B. S. Safina, J. Li, B. Zhang, C. Chabot, S. Do, L. Lee, J. Oeh, D. Sampath, B. B. Lee, K. Lin, B. M. Liederer and N. J. Skelton. Discovery and preclinical pharmacology of a selective ATP-competitive Akt inhibitor (GDC-0068) for the treatment of human tumors. J Med Chem. 2012. 55:8110-8127.

Bugliani, M., R. Liechti, H. Cheon, M. Suleiman, L. Marselli, C. Kirkpatrick, F. Filipponi, U. Boggi, I. Xenarios, F. Syed, L. Ladriere, C. Wollheim, M. S. Lee and P. Marchetti. Microarray analysis of isolated human islet transcriptome in type 2 diabetes and the role of the ubiquitin-proteasome system in pancreatic beta cell dysfunction. Mol Cell Endocrinol. 2013. 367:1-10.

Canale, C., S. Seghezza, S. Vilasi, R. Carrotta, D. Bulone, A. Diaspro, P. L. San Biagio and S. Dante. Different effects of Alzheimer's peptide Abeta(1-40) oligomers and fibrils on supported lipid membranes. Biophys Chem. 2013. 182:23-29.

Carnero, A. and J. M. Paramio. The PTEN/PI3K/AKT Pathway in vivo, Cancer Mouse Models. Front Oncol. 2014. 4:252.

Chen, H. J., J. C. Mitchell, S. Novoselov, J. Miller, A. L. Nishimura, E. L. Scotter, C. A. Vance, M. E. Cheetham and C. E. Shaw. The heat shock response plays an important role in TDP-43 clearance: evidence for dysfunction in amyotrophic lateral sclerosis. Brain. 2016. 139:1417-1432.

Chen, Y., B. Wang, D. Liu, J. J. Li, Y. Xue, K. Sakata, L. Q. Zhu, S. A. Heldt, H. Xu and F. F. Liao. Hsp90 chaperone inhibitor 17-AAG attenuates Abeta-induced synaptic toxicity and memory impairment. J Neurosci. 2014. 34:2464-2470.

Chien, V., J. F. Aitken, S. Zhang, C. M. Buchanan, A. Hickey, T. Brittain, G. J. Cooper and K. M. Loomes. The chaperone proteins HSP70, HSP40/DnaJ and GRP78/BiP suppress misfolding and formation of beta-sheet-containing aggregates by human amylin: a potential role for defective chaperone biology in Type 2 diabetes. Biochem J. 2010. 432:113-121.

Chiti, F. and C. M. Dobson. Protein Misfolding, Amyloid Formation, and Human Disease: A Summary of

Progress Over the Last Decade. Annu Rev Biochem. 2017. 86:27-68.

Chung, J., A. K. Nguyen, D. C. Henstridge, A. G. Holmes, M. H. Chan, J. L. Mesa, G. I. Lancaster, R. J. Southgate, C. R. Bruce, S. J. Duffy, I. Horvath, R. Mestril, M. J. Watt, P. L. Hooper, B. A. Kingwell, L. Vigh, A. Hevener and M. A. Febbraio. HSP72 protects against obesity-induced insulin resistance. Proc Natl Acad Sci U S A. 2008. 105:1739-1744.

Dai, C. and S. B. Sampson. HSF1: Guardian of Proteostasis in Cancer. Trends Cell Biol. 2016. 26:17-28.

Dai, C., S. Santagata, Z. Tang, J. Shi, J. Cao, H. Kwon, R. T. Bronson, L. Whitesell and S. Lindquist. Loss of tumor suppressor NF1 activates HSF1 to promote carcinogenesis. J Clin Invest. 2012. 122:3742-3754.

Dai, C., L. Whitesell, A. B. Rogers and S. Lindquist. Heat shock factor 1 is a powerful multifaceted modifier of carcinogenesis. Cell. 2007. 130:1005-1018.

Dai, R., W. Frejtag, B. He, Y. Zhang and N. F. Mivechi. c-Jun NH2-terminal kinase targeting and phosphorylation of heat shock factor-1 suppress its transcriptional activity. J Biol Chem. 2000. 275:18210-18218.

Dai, S., Z. Tang, J. Cao, W. Zhou, H. Li, S. Sampson and C. Dai. Suppression of the HSF1-mediated proteotoxic stress response by the metabolic stress sensor AMPK. EMBO J. 2015. 34:275-293.

Demuro, A., E. Mina, R. Kayed, S. C. Milton, I. Parker and C. G. Glabe. Calcium dysregulation and membrane disruption as a ubiquitous neurotoxic mechanism of soluble amyloid oligomers. J Biol Chem. 2005. 280:17294-17300.

Donnelly, N. and Z. Storchova. Aneuploidy and proteotoxic stress in cancer. Mol Cell Oncol. 2015. 2:e976491.

Engelman, J. A., J. Luo and L. C. Cantley. The evolution of phosphatidylinositol 3-kinases as regulators of growth and metabolism. Nat Rev Genet. 2006. 7:606-619.

Fernandez-Busquets, X. Amyloid fibrils in neurodegenerative diseases: villains or heroes? Future Med

Chem. 2013. 5:1903-1906.

Fujimoto, M., E. Takaki, T. Hayashi, Y. Kitaura, Y. Tanaka, S. Inouye and A. Nakai. Active HSF1 significantly suppresses polyglutamine aggregate formation in cellular and mouse models. J Biol Chem. 2005. 280:34908-34916.

Georganopoulou, D. G., L. Chang, J. M. Nam, C. S. Thaxton, E. J. Mufson, W. L. Klein and C. A. Mirkin. Nanoparticle-based detection in cerebral spinal fluid of a soluble pathogenic biomarker for Alzheimer's disease. Proc Natl Acad Sci U S A. 2005. 102:2273-2276.

Geula, C., C. K. Wu, D. Saroff, A. Lorenzo, M. Yuan and B. A. Yankner. Aging renders the brain vulnerable to amyloid beta-protein neurotoxicity. Nat Med. 1998. 4:827-831.

Girych, M., G. Gorbenko, I. Maliyov, V. Trusova, C. Mizuguchi, H. Saito and P. Kinnunen. Combined thioflavin T-Congo red fluorescence assay for amyloid fibril detection. Methods Appl Fluoresc. 2016. 4:034010.

Green, S., C. L. Trejo and M. McMahon. PIK3CA(H1047R) Accelerates and Enhances KRAS(G12D)-Driven Lung Tumorigenesis. Cancer Res. 2015. 75:5378-5391.

Gremer, L., D. Scholzel, C. Schenk, E. Reinartz, J. Labahn, R. B. G. Ravelli, M. Tusche, C. Lopez-Iglesias, W. Hoyer, H. Heise, D. Willbold and G. F. Schroder. Fibril structure of amyloid-beta(1-42) by cryo-electron microscopy. Science. 2017. 358:116-119.

Gu, J., W. Ou, L. Huang, J. Wu, S. Li, J. Xu, J. Feng, B. Liu and Y. Zhou. PTEN expression is associated with the outcome of lung cancer: evidence from a meta-analysis. Minerva Med. 2016. 107:342-351.

Guo, J. N., L. Y. Tian, W. Y. Liu, J. Mu and D. Zhou. Activation of the Akt/mTOR signaling pathway: A potential response to long-term neuronal loss in the hippocampus after sepsis. Neural Regen Res. 2017. 12:1832-1842.

Hayashida, N., M. Fujimoto, K. Tan, R. Prakasam, T. Shinkawa, L. Li, H. Ichikawa, R. Takii and A. Nakai. Heat shock factor 1 ameliorates proteotoxicity in cooperation with the transcription factor NFAT. EMBO J. 2010. 29:3459-3469.

Hayashida, N., S. Inouye, M. Fujimoto, Y. Tanaka, H. Izu, E. Takaki, H. Ichikawa, J. Rho and A. Nakai. A novel HSF1-mediated death pathway that is suppressed by heat shock proteins. EMBO J. 2006. 25:4773-4783.

Hayden, E. Y. and D. B. Teplow. Amyloid beta-protein oligomers and Alzheimer's disease. Alzheimers Res Ther. 2013. 5:60.

Hentze, N., L. Le Breton, J. Wiesner, G. Kempf and M. P. Mayer. Molecular mechanism of thermosensory function of human heat shock transcription factor Hsf1. Elife. 2016. 5:

Hermida, M. A., J. Dinesh Kumar and N. R. Leslie. GSK3 and its interactions with the PI3K/AKT/mTOR signalling network. Adv Biol Regul. 2017. 65:5-15.

Holmberg, C. I., V. Hietakangas, A. Mikhailov, J. O. Rantanen, M. Kallio, A. Meinander, J. Hellman, N. Morrice, C. MacKintosh, R. I. Morimoto, J. E. Eriksson and L. Sistonen. Phosphorylation of serine 230 promotes inducible transcriptional activity of heat shock factor 1. EMBO J. 2001. 20:3800-3810.

Huang, C., J. Wu, L. Xu, J. Wang, Z. Chen and R. Yang. Regulation of HSF1 protein stabilization: An updated review. Eur J Pharmacol. 2018. 822:69-77.

Huang, X., S. Wullschleger, N. Shpiro, V. A. McGuire, K. Sakamoto, Y. L. Woods, W. McBurnie, S. Fleming and D. R. Alessi. Important role of the LKB1-AMPK pathway in suppressing tumorigenesis in PTEN-deficient mice. Biochem J. 2008. 412:211-221.

Ingenwerth, M., E. Noichl, A. Stahr, H. W. Korf, H. Reinke and C. von Gall. Heat Shock Factor 1 Deficiency Affects Systemic Body Temperature Regulation. Neuroendocrinology. 2016. 103:605-615.

Jiang, Y. Q., X. L. Wang, X. H. Cao, Z. Y. Ye, L. Li and W. Q. Cai. Increased heat shock transcription factor 1 in the cerebellum reverses the deficiency of Purkinje cells in Alzheimer's disease. Brain Res. 2013. 1519:105-111.

Karakas, B., K. E. Bachman and B. H. Park. Mutation of the PIK3CA oncogene in human cancers. Br J Cancer. 2006. 94:455-459.

Kaushik, S. and A. M. Cuervo. Proteostasis and aging. Nat Med. 2015. 21:1406-1415.

Kayed, R., E. Head, F. Sarsoza, T. Saing, C. W. Cotman, M. Necula, L. Margol, J. Wu, L. Breydo, J. L. Thompson, S. Rasool, T. Gurlo, P. Butler and C. G. Glabe. Fibril specific, conformation dependent antibodies recognize a generic epitope common to amyloid fibrils and fibrillar oligomers that is absent in prefibrillar oligomers. Mol Neurodegener. 2007. 2:18.

Kechagioglou, P., R. M. Papi, X. Provatopoulou, E. Kalogera, E. Papadimitriou, P. Grigoropoulos, A. Nonni, G. Zografos, D. A. Kyriakidis and A. Gounaris. Tumor suppressor PTEN in breast cancer: heterozygosity, mutations and protein expression. Anticancer Res. 2014. 34:1387-1400.

Kim, E., B. Wang, N. Sastry, E. Masliah, P. T. Nelson, H. Cai and F. F. Liao. NEDD4-mediated HSF1 degradation underlies alpha-synucleinopathy. Hum Mol Genet. 2016. 25:211-222.

Kim, J. G., S. C. Lee, O. H. Kim, K. H. Kim, K. Y. Song, S. K. Lee, B. J. Choi, W. Jeong and S. J. Kim. HSP90 inhibitor 17-DMAG exerts anticancer effects against gastric cancer cells principally by altering oxidant-antioxidant balance. Oncotarget. 2017. 8:56473-56489.

Kim, S. A., J. H. Yoon, S. H. Lee and S. G. Ahn. Polo-like kinase 1 phosphorylates heat shock transcription factor 1 and mediates its nuclear translocation during heat stress. J Biol Chem. 2005. 280:12653-12657.

Kim, Y. E., M. S. Hipp, A. Bracher, M. Hayer-Hartl and F. U. Hartl. Molecular chaperone functions in protein folding and proteostasis. Annu Rev Biochem. 2013. 82:323-355.

Klaips, C. L., G. G. Jayaraj and F. U. Hartl. Pathways of cellular proteostasis in aging and disease. J Cell Biol. 2018. 217:51-63.

Knobbe, C. B., V. Lapin, A. Suzuki and T. W. Mak. The roles of PTEN in development, physiology and tumorigenesis in mouse models: a tissue-by-tissue survey. Oncogene. 2008. 27:5398-5415.

Kondo, N., M. Katsuno, H. Adachi, M. Minamiyama, H. Doi, S. Matsumoto, Y. Miyazaki, M. Iida, G. Tohnai, H. Nakatsuji, S. Ishigaki, Y. Fujioka, H. Watanabe, F. Tanaka, A. Nakai and G. Sobue. Heat shock factor-1 influences pathological lesion distribution of polyglutamine-induced neurodegeneration. Nat Commun. 2013. 4:1405.

Kone, M., T. J. Pullen, G. Sun, M. Ibberson, A. Martinez-Sanchez, S. Sayers, M. S. Nguyen-Tu, C. Kantor, A. Swisa, Y. Dor, T. Gorman, J. Ferrer, B. Thorens, F. Reimann, F. Gribble, J. A. McGinty, L. Chen, P. M. French, F. Birzele, T. Hildebrandt, I. Uphues and G. A. Rutter. LKB1 and AMPK differentially regulate pancreatic beta-cell identity. FASEB J. 2014. 28:4972-4985.

Labbadia, J. and R. I. Morimoto. The biology of proteostasis in aging and disease. Annu Rev Biochem. 2015. 84:435-464.

Laplante, M. and D. M. Sabatini. mTOR signaling in growth control and disease. Cell. 2012. 149:274-293.
Lee, Y. H., M. A. Magnuson, V. Muppala and S. S. Chen. Liver-specific reactivation of the inactivated Hnf-1alpha gene: elimination of liver dysfunction to establish a mouse MODY3 model. Mol Cell Biol. 2003. 23:923-932.

Lenting, K., R. Verhaak, M. Ter Laan, P. Wesseling and W. Leenders. Glioma: experimental models and reality. Acta Neuropathol. 2017. 133:263-282.

Lesche, R., M. Groszer, J. Gao, Y. Wang, A. Messing, H. Sun, X. Liu and H. Wu. Cre/loxP-mediated inactivation of the murine Pten tumor suppressor gene. Genesis. 2002. 32:148-149.

Liangliang, X., H. Yonghui, E. Shunmei, G. Shoufang, Z. Wei and Z. Jiangying. Dominant-positive HSF1 decreases alpha-synuclein level and alpha-synuclein-induced toxicity. Mol Biol Rep. 2010. 37:1875-1881.

Liao, Y., Y. Xue, L. Zhang, X. Feng, W. Liu and G. Zhang. Higher heat shock factor 1 expression in tumor stroma predicts poor prognosis in esophageal squamous cell carcinoma patients. J Transl Med. 2015. 13:338.

Lorenzo, A. and B. A. Yankner. Beta-amyloid neurotoxicity requires fibril formation and is inhibited by congo red. Proc Natl Acad Sci U S A. 1994. 91:12243-12247.

Makker, A., M. M. Goel and A. A. Mahdi. PI3K/PTEN/Akt and TSC/mTOR signaling pathways, ovarian dysfunction, and infertility: an update. J Mol Endocrinol. 2014. 53:R103-118.

Manning, B. D. and A. Toker. AKT/PKB Signaling: Navigating the Network. Cell. 2017. 169:381-405.

Martinelli, E., F. Morgillo, T. Troiani and F. Ciardiello. Cancer resistance to therapies against the EGFR-RAS-RAF pathway: The role of MEK. Cancer Treat Rev. 2017. 53:61-69.

Martins, P. M. True and apparent inhibition of amyloid fibril formation. Prion. 2013. 7:136-139.

Mattson, M. P., B. Cheng, D. Davis, K. Bryant, I. Lieberburg and R. E. Rydel. beta-Amyloid peptides destabilize calcium homeostasis and render human cortical neurons vulnerable to excitotoxicity. J Neurosci. 1992. 12:376-389.

Mendillo, M. L., S. Santagata, M. Koeva, G. W. Bell, R. Hu, R. M. Tamimi, E. Fraenkel, T. A. Ince, L. Whitesell and S. Lindquist. HSF1 drives a transcriptional program distinct from heat shock to support highly malignant human cancers. Cell. 2012. 150:549-562.

Meyer, D. S., S. Koren, C. Leroy, H. Brinkhaus, U. Muller, I. Klebba, M. Muller, R. D. Cardiff and M. Bentires-Alj. Expression of PIK3CA mutant E545K in the mammary gland induces heterogeneous tumors but is less potent than mutant H1047R. Oncogenesis. 2013. 2:e74.

Min, J. N., L. Huang, D. B. Zimonjic, D. Moskophidis and N. F. Mivechi. Selective suppression of lymphomas by functional loss of Hsf1 in a p53-deficient mouse model for spontaneous tumors. Oncogene. 2007. 26:5086-5097.

Mirzaa, G. M., J. B. Riviere and W. B. Dobyns. Megalencephaly syndromes and activating mutations in the PI3K-AKT pathway: MPPH and MCAP. Am J Med Genet C Semin Med Genet. 2013. 163C:122-130.

Morimoto, R. Creating a path from the heat shock response to therapeutics of protein-folding diseases: an interview with Rick Morimoto. Dis Model Mech. 2014. 7:5-8.

Morimoto, R. I. Heat shock: the role of transient inducible responses in cell damage, transformation, and differentiation. Cancer Cells. 1991. 3:295-301.

Morimoto, R. I. The heat shock response: systems biology of proteotoxic stress in aging and disease. Cold Spring Harb Symp Quant Biol. 2011. 76:91-99.

Outeiro, T. F. Amyloidogenesis: FlAsH illuminates Abeta aggregation. Nat Chem Biol. 2011. 7:581-582.
Ow, S. Y. and D. E. Dunstan. A brief overview of amyloids and Alzheimer's disease. Protein Sci. 2014. 23:1315-1331.

Pal, I. and M. Mandal. PI3K and Akt as molecular targets for cancer therapy: current clinical outcomes. Acta Pharmacol Sin. 2012. 33:1441-1458.

Porat, Y., A. Abramowitz and E. Gazit. Inhibition of amyloid fibril formation by polyphenols: structural similarity and aromatic interactions as a common inhibition mechanism. Chem Biol Drug Des. 2006. 67:27-37.

Regitz, C., E. Fitzenberger, F. L. Mahn, L. M. Dussling and U. Wenzel. Resveratrol reduces amyloid-beta (Abeta(1)(-)(4)(2))-induced paralysis through targeting proteostasis in an Alzheimer model of Caenorhabditis elegans. Eur J Nutr. 2016. 55:741-747.

Riviere, J. B., G. M. Mirzaa, B. J. O'Roak, M. Beddaoui, D. Alcantara, R. L. Conway, J. St-Onge, J. A. Schwartzentruber, K. W. Gripp, S. M. Nikkel, T. Worthylake, C. T. Sullivan, T. R. Ward, H. E. Butler, N. A. Kramer, B. Albrecht, C. M. Armour, L. Armstrong, O. Caluseriu, C. Cytrynbaum, B. A. Drolet, A. M. Innes, J. L. Lauzon, A. E. Lin, G. M. Mancini, W. S. Meschino, J. D. Reggin, A. K. Saggar, T. Lerman-Sagie, G. Uyanik, R. Weksberg, B. Zirn, C. L. Beaulieu, C. Finding of Rare Disease Genes Canada, J. Majewski, D. E. Bulman, M. O'Driscoll, J. Shendure, J. M. Graham, Jr., K. M. Boycott and W. B. Dobyns. De novo germline and postzygotic mutations in AKT3, PIK3R2 and PIK3CA cause a spectrum of related megalencephaly syndromes. Nat Genet. 2012. 44:934-940.

Ronnebaum, S. M., C. Patterson and J. C. Schisler. Minireview: hey U(PS): metabolic and proteolytic homeostasis linked via AMPK and the ubiquitin proteasome system. Mol Endocrinol. 2014. 28:1602-1615.
Rourke, J. L., Q. Hu and R. A. Screaton. AMPK and Friends: Central Regulators of beta Cell Biology. Trends Endocrinol Metab. 2018. 29:111-122.

Samuels, Y. and T. Waldman. Oncogenic mutations of PIK3CA in human cancers. Curr Top Microbiol Immunol. 2010. 347:21-41.

Sansregret, L. and C. Swanton. The Role of Aneuploidy in Cancer Evolution. Cold Spring Harb Perspect Med. 2017. 7:

Santagata, S., R. Hu, N. U. Lin, M. L. Mendillo, L. C. Collins, S. E. Hankinson, S. J. Schnitt, L. Whitesell, R. M. Tamimi, S. Lindquist and T. A. Ince. High levels of nuclear heat-shock factor 1 (HSF1) are associated with poor prognosis in breast cancer. Proc Natl Acad Sci U S A. 2011. 108:18378-18383.

Scheper, W., D. A. Nijholt and J. J. Hoozemans. The unfolded protein response and proteostasis in Alzheimer disease: preferential activation of autophagy by endoplasmic reticulum stress. Autophagy. 2011. 7:910-911.

Soncin, F., X. Zhang, B. Chu, X. Wang, A. Asea, M. Ann Stevenson, D. B. Sacks and S. K. Calderwood. Transcriptional activity and DNA binding of heat shock factor-1 involve phosphorylation on threonine 142

by CK2. Biochem Biophys Res Commun. 2003. 303:700-706.

Srinivasan, L., Y. Sasaki, D. P. Calado, B. Zhang, J. H. Paik, R. A. DePinho, J. L. Kutok, J. F. Kearney, K. L. Otipoby and K. Rajewsky. PI3 kinase signals BCR-dependent mature B cell survival. Cell. 2009. 139:573-586.

Steele, A. D., G. Hutter, W. S. Jackson, F. L. Heppner, A. W. Borkowski, O. D. King, G. J. Raymond, A. Aguzzi and S. Lindquist. Heat shock factor 1 regulates lifespan as distinct from disease onset in prion disease. Proc Natl Acad Sci U S A. 2008. 105:13626-13631.

Swan, C. L. and L. Sistonen. Cellular stress response cross talk maintains protein and energy homeostasis. EMBO J. 2015. 34:267-269.

Tanaka, K. and N. Matsuda. Proteostasis and neurodegeneration: the roles of proteasomal degradation and autophagy. Biochim Biophys Acta. 2014. 1843:197-204.

Tang, J., M. Lu and D. Tang. Target-initiated impedimetric proximity ligation assay with DNAzyme design for in situ amplified biocatalytic precipitation. Analyst. 2014. 139:2998-3001.

Tang, Z. and C. Dai. Visualization of RAS/MAPK Signaling In Situ by the Proximity Ligation Assay (PLA). Methods Mol Biol. 2017. 1487:195-201.

Tang, Z., S. Dai, Y. He, R. A. Doty, L. D. Shultz, S. B. Sampson and C. Dai. MEK guards proteome stability and inhibits tumor-suppressive amyloidogenesis via HSF1. Cell. 2015. 160:729-744.

Tofoleanu, F. and N. V. Buchete. Alzheimer Abeta peptide interactions with lipid membranes: fibrils, oligomers and polymorphic amyloid channels. Prion. 2012. 6:339-345.

Tolcher, A., J. Goldman, A. Patnaik, K. P. Papadopoulos, P. Westwood, C. S. Kelly, W. Bumgardner, L. Sams, S. Geeganage, T. Wang, A. R. Capen, J. Huang, S. Joseph, J. Miller, K. A. Benhadji, L. H. Brail and

L. S. Rosen. A phase I trial of LY2584702 tosylate, a p70 S6 kinase inhibitor, in patients with advanced solid tumours. Eur J Cancer. 2014. 50:867-875.

Tong, Y., Y. Li, H. Gu, C. Wang, F. Liu, Y. Shao and F. Li. HSF1, in association with MORC2, downregulates ArgBP2 via the PRC2 family in gastric cancer cells. Biochim Biophys Acta. 2018.

Trisciuoglio, D., A. Iervolino, G. Zupi and D. Del Bufalo. Involvement of PI3K and MAPK signaling in bcl-2-induced vascular endothelial growth factor expression in melanoma cells. Mol Biol Cell. 2005. 16:4153-4162.

Tycko, R. Physical and structural basis for polymorphism in amyloid fibrils. Protein Sci. 2014. 23:1528-1539.

Umezawa, S., T. Higurashi and A. Nakajima. AMPK: Therapeutic Target for Diabetes and Cancer Prevention. Curr Pharm Des. 2017. 23:3629-3644.

Vihervaara, A., C. Sergelius, J. Vasara, M. A. Blom, A. N. Elsing, P. Roos-Mattjus and L. Sistonen. Transcriptional response to stress in the dynamic chromatin environment of cycling and mitotic cells. Proc Natl Acad Sci U S A. 2013. 110:E3388-3397.

Vihervaara, A. and L. Sistonen. HSF1 at a glance. J Cell Sci. 2014. 127:261-266.

Viola, K. L. and W. L. Klein. Amyloid beta oligomers in Alzheimer's disease pathogenesis, treatment, and diagnosis. Acta Neuropathol. 2015. 129:183-206.

Voukkalis, N., M. Koutroumani, C. Zarkadas, E. Nikolakaki, M. Vlassi and T. Giannakouros. SRPK1 and Akt Protein Kinases Phosphorylate the RS Domain of Lamin B Receptor with Distinct Specificity: A Combined Biochemical and In Silico Approach. PLoS One. 2016. 11:e0154198.

Wang, M., H. Xin, W. Tang, Y. Li, Z. Zhang, L. Fan, L. Miao, B. Tan, X. Wang and Y. Z. Zhu. AMPK Serves as a Therapeutic Target Against Anemia of Inflammation. Antioxid Redox Signal. 2017. 27:251-

268.

Wentink, M., V. Dalm, A. C. Lankester, P. A. van Schouwenburg, L. Scholvinck, T. Kalina, R. Zachova, A. Sediva, A. Lambeck, I. Pico-Knijnenburg, J. J. van Dongen, M. Pac, E. Bernatowska, M. van Hagen, G. Driessen and M. van der Burg. Genetic defects in PI3Kdelta affect B-cell differentiation and maturation leading to hypogammaglobulineamia and recurrent infections. Clin Immunol. 2017. 176:77-86.

Winder, A., K. Unno, Y. Yu, J. Lurain and J. J. Kim. The allosteric AKT inhibitor, MK2206, decreases tumor growth and invasion in patient derived xenografts of endometrial cancer. Cancer Biol Ther. 2017. 0.

Winner, B., R. Jappelli, S. K. Maji, P. A. Desplats, L. Boyer, S. Aigner, C. Hetzer, T. Loher, M. Vilar, S. Campioni, C. Tzitzilonis, A. Soragni, S. Jessberger, H. Mira, A. Consiglio, E. Pham, E. Masliah, F. H. Gage and R. Riek. In vivo demonstration that alpha-synuclein oligomers are toxic. Proc Natl Acad Sci U S A. 2011. 108:4194-4199.

Wong, K. K. Recent developments in anti-cancer agents targeting the Ras/Raf/ MEK/ERK pathway. Recent Pat Anticancer Drug Discov. 2009. 4:28-35.

Xi, C., Y. Hu, P. Buckhaults, D. Moskophidis and N. F. Mivechi. Heat shock factor Hsf1 cooperates with ErbB2 (Her2/Neu) protein to promote mammary tumorigenesis and metastasis. J Biol Chem. 2012. 287:35646-35657.

Yang, H., M. H. Lee, I. Park, H. Jeon, J. Choi, S. Seo, S. W. Kim, G. Y. Koh, K. S. Park and D. H. Lee. HSP90 inhibitor (NVP-AUY922) enhances the anti-cancer effect of BCL-2 inhibitor (ABT-737) in small cell lung cancer expressing BCL-2. Cancer Lett. 2017. 411:19-26.

Yi, K. H. and J. Lauring. Recurrent AKT mutations in human cancers: functional consequences and effects on drug sensitivity. Oncotarget. 2016. 7:4241-4251.

Zadra, G., J. L. Batista and M. Loda. Dissecting the Dual Role of AMPK in Cancer: From Experimental to Human Studies. Mol Cancer Res. 2015. 13:1059-1072.

Zhang, X., B. Jin and C. Huang. The PI3K/Akt pathway and its downstream transcriptional factors as targets for chemoprevention. Curr Cancer Drug Targets. 2007. 7:305-316.

Zhang, Y., A. Murshid, T. Prince and S. K. Calderwood. Protein kinase A regulates molecular chaperone transcription and protein aggregation. PLoS One. 2011. 6:e28950.

Zhong, J. RAS and downstream RAF-MEK and PI3K-AKT signaling in neuronal development, function and dysfunction. Biol Chem. 2016. 397:215-222.

Zhou, W., J. Zhang and A. I. Marcus. LKB1 Tumor Suppressor: Therapeutic Opportunities Knock when LKB1 Is Inactivated. Genes Dis. 2014. 1:64-74.

Zhuo, L., M. Theis, I. Alvarez-Maya, M. Brenner, K. Willecke and A. Messing. hGFAP-cre transgenic mice for manipulation of glial and neuronal function in vivo. Genesis. 2001. 31:85-94.

Zraika, S., K. Aston-Mourney, P. Marek, R. L. Hull, P. S. Green, J. Udayasankar, S. L. Subramanian, D. P. Raleigh and S. E. Kahn. Neprilysin impedes islet amyloid formation by inhibition of fibril formation rather than peptide degradation. J Biol Chem. 2010. 285:18177-18183.

BIOGRAPHY OF THE AUTHOR

Zijian Tang was born in Wuhan, Hubei, China on September 29, 1983. He was raised in Wuhan, Hubei, China and graduated from Huagong High School in 2002. He attended the University of Wuhan and graduated in 2006 with a Bachelor's degree in Biology. He obtained his Master Degree of Biochemistry and Molecular Biology in University of Wuhan in the summer of 2008. Then he came to Maine and entered the Biochemistry and Molecular Biology program at The University of Maine in the fall of 2012. Zijian Tang is a candidate for the Doctor of Philosophy degree in Biochemistry and Molecular Biology from the University of Maine in May 2018.